HHS Public Access

Author manuscript

J Mech Phys Solids. Author manuscript; available in PMC 2021 June 01.

Published in final edited form as:

J Mech Phys Solids. 2020 June ; 139: . doi:10.1016/j.jmps.2020.103936.

A Coupled Mass Transport and Deformation Theory of Multi-constituent Tumor Growth

Danial Faghihi[1,*], **Xinzeng Feng**[2], **Ernesto A. B. F. Lima**[2], **J. Tinsley Oden**[2,3,4,5,9], **Thomas E. Yankeelov**[2,6,7,8,9]

[1]Department of Mechanical and Aerospace Engineering, University at Buffalo

[2]Oden Institute for Computational Engineering and Sciences

[3]Department of Aerospace Engineering and Engineering Mechanics, The University of Texas at Austin

[4]Department of Mathematics, The University of Texas at Austin

[5]Department of Computer Science, The University of Texas at Austin

[6]Department of Biomedical Engineering, The University of Texas at Austin

[7]Department of Diagnostic Medicine, The University of Texas at Austin

[8]Department of Oncology, The University of Texas at Austin

[9]Livestrong Cancer Institutes, The University of Texas at Austin

Abstract

We develop a general class of thermodynamically consistent, continuum models based on mixture theory with phase effects that describe the behavior of a mass of multiple interacting constituents. The constituents consist of solid species undergoing large elastic deformations and compressible viscous fluids. The fundamental building blocks framing the mixture theories consist of the mass balance law of diffusing species and microscopic (cellular scale) and macroscopic (tissue scale) force balances, as well as energy balance and the entropy production inequality derived from the first and second laws of thermodynamics. A general phase-field framework is developed by

[*]Corresponding author. Assistant Professor, Department of Mechanical and Aerospace Engineering, University at Buffalo, Buffalo, NY. danialfa@buffalo.edu.

Credit Author Statement:

Danial Faghihi: Conceptualization, Methodology, Software, Formal analysis, Writing - Original Draft, Writing - Review & Editing, Visualization.

Xinzeng Feng: Methodology, Writing - Original Draft, Visualization, Formal analysis. Ernesto A. B. F. Lima: Methodology, Software, Formal analysis, Writing - Original Draft, Writing - Review & Editing, Visualization.

J. Tinsley Oden: Methodology, Validation, Resources, Writing - Original Draft, Writing - Review & Editing, Supervision, Project administration.

Thomas E. Yankeelov: Validation, Resources, Writing - Original Draft, Writing - Review & Editing, Supervision, Project administration, Funding acquisition.

Declaration of interests

The authors declare that they have no known competing financial interests or personal relationships that could have appeared to influence the work reported in this paper.

closing the system through postulating constitutive equations (i.e., specific forms of free energy and rate of dissipation potentials) to depict the growth of tumors in a microenvironment. A notable feature of this theory is that it contains a unified continuum mechanics framework for addressing the interactions of multiple species evolving in both space and time and involved in biological growth of soft tissues (e.g., tumor cells and nutrients). The formulation also accounts for the regulating roles of the mechanical deformation on the growth of tumors, through a physically and mathematically consistent coupled diffusion and deformation framework. A new algorithm for numerical approximation of the proposed model using mixed finite elements is presented. The results of numerical experiments indicate that the proposed theory captures critical features of avascular tumor growth in the various microenvironment of living tissue, in agreement with the experimental studies in the literature.

Keywords

Mixture theory; Phase-field; Hyperelastic solid; Biochemomechanical coupling; Tumor growth

1 Introduction

There is a vast and growing literature on mathematical and computational models of the physical and biological processes involved in the initiation, development, and growth of cancer [2, 12, 61, 80, 121, 131, 137, 149, 167]. Most tumor models can be categorized as either a discrete cell-based model, or a continuum model. The continuum approach considers the average of the global cell population behavior [35, 96, 120, 160, 164], while discrete approaches track and update individual cell dynamics using a prescribed set of biophysical rules [19, 82, 135, 154]. Due to the rapid increase in the computational cost of discrete methods with the number of cells modeled, continuum methods are often favored for providing predictions in *in vivo* systems for events at experimentally observable spatial and temporal scales.

Fundamental theoretical challenges in the continuum modeling of tumor growth arise in describing the associations between gain and loss of mass and stresses induced by cancer cell proliferation and apoptosis, as well as the effect of a nonuniform microenvironment. Extensive efforts over the last two decades have resulted in various theoretical approaches [4, 46, 76, 106, 121, 165, 166]. Although these previous efforts address several open issues in understanding, simulating, and predicting tumor growth, the development of a unified mathematical framework for modeling the growth process is still a central challenge in biomechanics [4].

Several continuum theories are based on the abstraction of a homogenized, single-constituent tumor [137, 165]. These purely mechanical models implicitly assume sources of mass supply to drive the growth of the tumor. Although these methods can yield self-consistent frameworks, they are incapable of accounting for important biophysical phenomena encountered in tumor progression including, for example, nutrient delivery by the surrounding tissues and consumption by tumor cells. A more realistic representation of a tumor growing in a microenvironment can be achieved through a framework based on

continuum theories of mixtures [24, 38, 120, 132] which naturally incorporate various solid and fluid constituents involved in the underlying biophysical phenomena. Mixture theory has been the focus of much research in mechanics for many years [23] as a basis for treating the behavior of porous media involving two or more interacting bodies. In mixture models of tumor growth, the governing equations consist of mass and momentum balance equations for each species, interphase mass, and momentum exchange, along with appropriate constitutive equations. Recently, multiphase mixture models have been developed to address heterogeneities in cell-phenotypes and the mechanical response of tumor phases (see, e.g., [8, 25, 28, 48, 49, 57, 111, 116, 139]). Phase-field models provide a general approach to modeling multiphase materials [22, 100], in which the interface between phases is handled automatically as a feature of the solution and represents boundary layers between phases. In general, such models are obtained by incorporating gradients of the order parameters, such as the concentrations of various constituents, in the free energy functionals of a multiphase material to approximate surface energies at interfaces. The most common model of this type is the Cahn-Hilliard model of binary phase separation [29] in which the free energy contains gradients in concentrations multiplied by parameters which characterize the thickness of the smoothed interfaces between the phases. Phase field models have provided important frameworks for characterizing microstructural evolution at the mesoscale [155], solidification [22], grain growth [112], dislocation dynamics [169], and self-assembly of block copolymers [32] among others. Recently, phase-field models have been applied to simulate tumor growth and decline [35, 96, 120, 164]. A multi-species framework allows for characterizing the interaction between (for example) the necrotic, apoptotic, quiescent, and proliferative cells present in solid, avascular tumors.

In addition to the underlying mathematical framework, another challenge in developing tumor growth models is simulating the mechanical cues to tumor cells alongside the biological and chemical factors. Experimental studies indicate that the mechanical stresses of the solid phase of a tumor play a vital role in the expansion, invasion, and metastasis of tumors [26, 78, 79, 91, 109, 147, 157]. These macroscopic stresses arise due to heterogeneous tumor growth as well as the effect of surrounding tissue confinement. While the generation of residual stresses from heterogeneous growth is significant in normal tissues such as arteries and mucosa [92, 93, 144, 150], the external stresses on tumors produced by the surrounding tissues can be more prominent than those incurred by the heterogeneous growth [4, 7]. The mechanical stresses moderate the development of solid tumors by compressing both the tumor and the associated vasculature. These effects result in lowering the proliferation rate and stimulating apoptosis of the cancer cells, as well as enhancing the invasiveness and metastatic potential of a tumor [72, 79, 113]. However, these mechano-chemo-biological mechanisms, which are determined by cell-cell and cell-microenvironment interactions, have not been adequately addressed by current theoretical continuum models [4, 46]. The majority of the previous investigations on modeling growth-induced stresses rely on phenomenological evolution equations of the growth-associated strains. Such assumptions result in models that fail to address the effect of microscale evolutions on the macroscopic stress and strain, and they are inadequate to characterize the mechanical aspects of the biological growth [4].

To overcome the above-mentioned modeling challenges, we develop a general class of thermodynamically consistent continuum models, based on mixture theory with diffuse interface effects, that describes the biomechanical behavior of a mass of N interacting constituents. M of these N constituents are solid species undergoing finite strain elastic deformation and growth, and NM can be compressible, Newtonian viscous fluids. A general phase-field framework is developed by considering the free energy and rate of dissipation potential as primary potentials and thermodynamic forces are derived considering the processes leading to energy storage and dissipation. The constitutive relations are deduced from specific forms of the Helmholtz free energy and rate of dissipation to simulate major features of avascular tumor growth in a microenvironment. Special attention is given to the mechanical cues detected by tumor cells and their effects on tumor progression. In this regard, a fully coupled deformation and mass transfer model is developed through physically and mathematically consistent construction. The proposed mathematical model is numerically solved using mixed finite elements, and several numerical experiments are conducted considering a system consists of four interacting constituents: tumor cells, healthy cells, nutrient-rich and nutrient-poor extracellular water. The numerical experiments indicate that the general diffusion-deformation framework proposed in this work enables simulating the significant mechano-chemo-biological features of avascular tumor growth in the various microenvironment of living tissue, in agreement with the experimental studies in the literature. In particular, the proposed model accounts for the growth of the proliferating tumor cells due to nutrient consumption, the directional movement of tumor cells towards the nutrient supply, and the surface tension stress due to cell-cell adhesion at the interface of tumor and healthy cells constituents. More importantly, this work enables simulating the significant inhibitory effect of the confinement induced by the surrounding tissues on the avascular tumor growth, using a new evolution equation of the growth deformation gradient derived from the mass transfer relations.

The rest of this contribution is organized as follows. Section 2 presents the theoretical development of the phase-field mixture theory, providing a framework for the proposed four-constituent tumor growth model, which is described in section 3. The results of numerical experiments designed to demonstrate the qualitative model prediction are described in section 4. The Discussion and Conclusions are given in section 5.

2 Theoretical Framework: Coupled Mass Transport and Deformation of Multi-species Mixtures

Our theoretical framework of tumor growth model is founded in the continuum theory of mixtures, advanced by Truesdell [151], Truesdell and Toupin [153], Bowen [23, 24], and Eringen and Ingram [42, 77]. Parallel developments of theories of porous media share many aspects of mixture theory for two- or three-phase materials, as can be seen in works such as those by de Boer [37, 38] among many others. The development of diffuse-interface models based on mixture theory involves an additional level of complexity due to the dynamical effects associated with changes in the volume fractions of the constituents [120, 132]. We follow the basic hypotheses of Truesdell and Noll [152] in developing a physically meaningful continuum theory. In this regard, the general theory governing a continuum

mixture of N constituents is developed based on the balance laws for mass, momentum, and energy as well as the inequality for entropy production. These laws are the fundamental building blocks on which to frame theories of material behavior. Then a general phase-field version is developed by closing the system with constitutive equations. In this regard, the free energy and rate of dissipation potential are considered as primary potentials, and thermodynamic forces are derived considering the processes leading to energy storage and dissipation.

2.1 A Continuum Theory of Mixture

In continuum mechanics, a body $\mathscr{B}$ is viewed as a set of material points that occupy subsets of Euclidean space as the motion of the body carries it through various configurations. It is a convention to choose one such region as a reference and refer to it as the reference configuration of $\mathscr{B}$. The material points of the body are identified with their positions $\mathbf{X}$. The underlying assumption of mixture theory is that a material body $\mathscr{B}$ consists of N constituent species that occupy a common part of physical space at the same time. The body undergoes a motion which maps the reference configuration $\mathscr{B}$ onto a current configuration $\mathscr{B}_t$, with the spatial position of material points at time t, given by $\mathbf{x} = \mathscr{X}(\mathbf{X}, t)$. In an N-species mixture the motion is defined by

$$\mathbf{x} = \mathscr{X}_\alpha(\mathbf{X}_\alpha, t), \tag{1}$$

where $\alpha = 1, 2, \cdots, N$ and $\mathbf{X}_\alpha$ is the position of the material points of the α-th constituent in its reference configuration. The deformation gradient is defined by

$$\mathbf{F}_\alpha := \frac{\partial \mathscr{X}_\alpha}{\partial \mathbf{X}_\alpha}. \tag{2}$$

Each spatial position $\mathbf{x}$ is occupied by N different constituents, and each constituent has a mass density, $\hat{\rho}_\alpha(\mathbf{x}, t)$, representing the mass of the α-th constituent per unit volume of the mixture at time t. The mass density of the mixture at a point $(\mathbf{x}, t)$ is defined as[1],

$$\rho(\mathbf{x}, t) = \sum_\alpha \hat{\rho}_\alpha(\mathbf{x}, t), \tag{3}$$

and the (partial) density, ρ_α, is

$$\hat{\rho}_\alpha(\mathbf{x}, t) = \rho_\alpha(\mathbf{x}, t)\phi_\alpha(\mathbf{x}, t), \tag{4}$$

representing the mass of α-th constituent per unit volume of the constituent. The mass concentration and volume fraction of the α-th constituent are defined respectively by,

[1]Throughout the formulation the subscript α is an index taking on values, $1 \le \alpha \le N$, unless otherwise specified, and we shall use the abbreviated notation $\sum_\alpha = \sum_{\alpha=1}^{N}$.

$$c_\alpha(\mathbf{x},t)=\frac{\hat{\rho}_\alpha(\mathbf{x},t)}{\rho(\mathbf{x},t)} \quad , \quad \phi_\alpha(\mathbf{x},t)=\frac{dv_\alpha}{dv}, \tag{5}$$

where dv is a differential volume containing the point $\mathbf{x}$, and dv_α is the proportion of volume occupied by constituent α. From (5) clearly,

$$\sum_\alpha c_\alpha = 1 \quad , \quad \sum_\alpha \phi_\alpha = 1\,. \tag{6}$$

In addition, the velocity of each constituent and the mixture velocity are defined as,

$$\mathbf{v}_\alpha(\mathbf{x},t)=\frac{\partial \mathcal{X}_\alpha(\mathbf{X}_\alpha,t)}{\partial t} \quad , \quad \mathbf{v}=\frac{1}{\rho}\sum_\alpha \rho_\alpha\phi_\alpha\mathbf{v}_\alpha\,. \tag{7}$$

The diffusion velocity for the α-th constituent is also defined by

$$\mathbf{p}_\alpha=\mathbf{v}_\alpha-\mathbf{v}, \quad \text{with} \quad \sum_\alpha \rho_\alpha\phi_\alpha\mathbf{p}_\alpha=0\,. \tag{8}$$

The velocity gradient of each constituent, $\mathbf{L}_\alpha = \nabla\cdot\mathbf{v}_\alpha$, can be split into symmetric, $\mathbf{D}_\alpha$, and skew-symmetric, $\mathbf{W}_\alpha$, parts in which,

$$\mathbf{D}_\alpha=\frac{1}{2}(\nabla\mathbf{v}_\alpha+\nabla\mathbf{v}_\alpha^T) \quad , \quad \mathbf{W}_\alpha=\frac{1}{2}(\nabla\mathbf{v}_\alpha-\nabla\mathbf{v}_\alpha^T)\,. \tag{9}$$

Finally, the link between Lagrangian and Eulerian descriptions in time derivatives can be made according to

$$\frac{d^\alpha\phi}{dt}=\frac{\partial\phi}{\partial t}+\mathbf{v}_\alpha\cdot\nabla\phi, \tag{10}$$

where $d^\alpha\phi/dt$ is the material time-derivative related to the motion of each constituent and ϕ is any differentiable function of $\mathbf{x}$ and t.

Each of the N species must satisfy its own balance laws consistent with the presence of interaction among constituents. The balance laws govern the behavior of a general mixture that must hold for all α, $1\le\alpha\le N$, are presented in the next sections.

2.2 Macroscopic and Microscopic Force Balances

Let $\mathscr{R}_t$ denote an arbitrary spatial region convecting within the body $\mathscr{B}$ at time t. The basic balance laws for linear and angular momentum assert that the net force and momentum on $\mathscr{R}_t$ are balanced by temporal changes in the linear and angular momentum of $\mathscr{R}_t$. In this regard, the balance of linear momentum for α-constituent in the mixture requires,

$$\frac{d^{\alpha}}{dt}\int_{\mathscr{R}_t}\rho_{\alpha}\phi_{\alpha}\mathbf{v}_{\alpha}\mathrm{d}V=\int_{\partial\mathscr{R}_t}\mathbf{T}_{\alpha}\,.\,\mathbf{n}\;\mathrm{d}A+\int_{\mathscr{R}_t}(\rho_{\alpha}\phi_{\alpha}\mathbf{b}_{\alpha})\mathrm{d}V, \tag{11}$$

where $\mathbf{T}_{\alpha}$ is the partial Cauchy stress tensor, $\mathbf{b}_{\alpha}$ is the body force per unit mass, $\mathbf{n}(\mathbf{x}, t)$ denotes the outward unit normal field on the boundary $\partial\mathscr{R}_t$, and dA and dV are differential surface and volume elements of $\partial\mathscr{R}_t$. Using the divergence theorem, and taking into account that (11) must hold for all spatial regions, leads to the *macroforce balance*,

$$\frac{d^{\alpha}\rho_{\alpha}\phi_{\alpha}\mathbf{v}_{\alpha}}{dt}=\nabla\cdot\mathbf{T}_{\alpha}+\rho_{\alpha}\phi_{\alpha}\mathbf{b}_{\alpha}\,. \tag{12}$$

In the case of nonpolar materials (neglecting, e.g., electromagnetic effects and micro-moments), the balance of angular momentum results in the relation,

$$\mathbf{T}_{\alpha}=\mathbf{T}_{\alpha}^{T} \tag{13}$$

so the partial Cauchy stress is symmetric.

To describe the phase dynamics in the mixture (following the arguments of [62]), in addition to local force balances, we postulate the existence of a set of microscopic forces that accompany the evolution of each order parameter (i.e., the volume fraction in the present formulation). These thermodynamical forces are termed “microscopic” because they are involved with phenomena that occur at a scale (e.g., cell level) smaller than macroscopic interactions (e.g., tissue level). The notion of microscopic forces has been successfully applied to to develop generalized frameworks such as strain gradient-plasticity theories [64, 158], generalized heat transfer [44], micromorphic approaches [16, 45], and mixture theories of porous media [59, 126].

The (micro-)kinematics of phase, ϕ_{α}, such as the phase separation and mixing of different components, is associated with three microforces per unit volume, including the internal microforce π_{α} and the external microforce τ_{α} that are associated with volume fraction[2] and the thermodynamic stress conjugate to the gradient of species volume fractions $\boldsymbol{\xi}_{\alpha}$ that represents a flux through the boundary $\partial\mathscr{R}_t$. These nonlocal forces are balanced through the following relation,

$$\int_{\partial\mathscr{R}_t}\boldsymbol{\xi}_{\alpha}\,.\,\mathbf{n}\;\mathrm{d}A+\int_{\mathscr{R}_t}\pi_{\alpha}\mathrm{d}V+\int_{\mathscr{R}_t}\pi_{\alpha}\mathrm{d}V=0\,. \tag{14}$$

Making use of the divergence theorem and the fact that $\mathscr{R}_t$ is arbitrary leads to the following *species microforce balance*,

[2]To simplify the notation, π_{α} and τ_{α} are defined as forces per unit volume. If these quantities are defined as forces per unit mass, they need to appear in (14) as $\rho_{\alpha}\phi_{\alpha}\pi_{\alpha}$ and $\rho_{\alpha}\phi_{\alpha}\tau_{\alpha}$ similar to the body force in (11).

$$\nabla \cdot \boldsymbol{\xi}_\alpha + \pi_\alpha + \tau_\alpha = 0\,. \tag{15}$$

The additional balance law (15) arises due to considering the volume fraction of each constituent as an independent kinematical quantity in the mixture theory. This force balance is essential in the theory of phase-field mixtures to account for the dynamical effects associated with changes in the volume fractions of the constituents, although it does not ordinarily arise in mixture theories. The general formulation described in this section leads to biological interpretations of microforces in tumor growth phenomena described in section 2.6[3] (See Appendix A for an alternative approach to determine the associated balance of macroscopic and microscopic forces using the principle of virtual power.)

2.3 Diffusing Species Mass Balance

The net mass of the diffusing species in the spatial region $\mathscr{R}_t$ is represented by $\int_{\mathscr{R}_t} \rho_\alpha \phi_\alpha \mathrm{d}V$. The species transport to $\mathscr{R}_t$ can be characterized by the rate at which the species is transported to $\mathscr{R}_t$ by diffusion across $\partial\mathscr{R}_t$ as well as the rate of transport to $\mathscr{R}_t$ by constituents external to the body. In this regard, species mass balance requires that,

$$\frac{d^\alpha}{dt}\int_{\mathscr{R}_t} \rho_\alpha \phi_\alpha \mathrm{d}V = -\int_{\partial\mathscr{R}_t} \mathbf{J}_\alpha \cdot \mathbf{n}\, \mathrm{d}A + \int_{\mathscr{R}_t} S_\alpha \mathrm{d}V, \tag{16}$$

where $\mathbf{J}_\alpha$ is the mass flux and S_α is external species mass supplied (a source term). Thus, (16) suggests that the mass-rate-of-change of the α-th component must balance with the net rate of generation of the α-th component in $\mathscr{R}_t$. Using the Reynolds' transport relation along with the divergence theorem, the local *species mass balance* is [43]

$$\frac{\partial \rho_\alpha \phi_\alpha}{\partial t} + \nabla \cdot (\rho_\alpha \phi_\alpha \mathbf{v}_\alpha) = S_\alpha - \nabla \cdot \mathbf{J}_\alpha\,. \tag{17}$$

The right-hand side of (17) is called the mass growth rate of the αth component [23].

2.4 Force and Mass Balance for the Mixture

The balance equations for the mixture, governing the motion of a single body, should follow the individual species balance equation summing over all constituents. Thus the continuum balance laws of the full mixture can be written as,

$$\rho \frac{d\mathbf{v}}{dt} = \nabla \cdot \mathbf{T} + \mathbf{b}, \tag{18}$$

[3] In theories of granular materials (e.g., Goodman and Cowin [59] and Passman, Nunziato, Walsh [118, 126]), the relation (15) is noted as the balance of equilibrated force. In the case of granular materials, the generalized microforces are physically interpreted as π_α being related to the pressure in the matrix acting on the voids and the material properties of the matrix, τ_α being related to an externally controlled pore pressure, and $\boldsymbol{\xi}_\alpha$ as being a stress-type quantity and associated with the inter-granular contact forces which influence the packing or fabric of the mixture [81, 86, 118, 126]. Additionally, in [118] the internal force π_α is decomposed into a force supply associated with the species α and a force interaction associated with the interaction of α-th species with all other constituents. For simplicity of notation, we avoid such decompositions.

$$\nabla \cdot \boldsymbol{\xi} + \pi + \tau = 0, \tag{19}$$

$$\frac{\partial \rho}{\partial t} + \nabla \cdot (\rho \mathbf{v}) = 0, \tag{20}$$

subject to the following constraints,

$$\begin{aligned} \mathbf{b} &= \frac{1}{\rho} \sum_{\alpha} \rho_{\alpha} \phi_{\alpha} \mathbf{b}_{\alpha}, \\ \sum_{\alpha} S_{\alpha} &= \sum_{\alpha} \nabla \cdot \mathbf{J}_{\alpha}, \\ \boldsymbol{\xi} &= \sum_{\alpha} \boldsymbol{\xi}_{\alpha}, \\ \pi &= \sum_{\alpha} \pi_{\alpha}, \\ \tau &= \sum_{\alpha} \tau_{\alpha} \\ \mathbf{T} &= \sum_{\alpha} \mathbf{T}_{\alpha} - \rho_{\alpha} \phi_{\alpha} \mathbf{p}_{\alpha} \otimes \mathbf{p}_{\alpha}. \end{aligned} \tag{21}$$

In the above relations, ρ, $\mathbf{T}$, $\mathbf{b}$, and $\mathbf{v}$ are the mass density, Cauchy stress, body force per unit mass, and velocity of the mixture, respectively.

2.5 Thermodynamics Derivation

2.5.1 The First Law: Balance of Energy—The first law of thermodynamics represents a balance between the internal energy of $\mathscr{R}_t$, the rate at which power is expended on $\mathscr{R}_t$, and the energy carried into $\mathscr{R}_t$ by species transport. In the present formulation, we consider isothermal processes (i.e., the heating $d\mathscr{Q} / dt \approx 0$) and assume that the kinetic energy is negligible. Defining the net internal energy of mixture as $\mathscr{E} = \int_{\mathscr{R}_t} \rho \varepsilon \mathrm{d}V$, with ε being the specific internal energy, the first law of thermodynamics is written as

$$\frac{d}{dt}\mathscr{E} = \mathscr{P}_{\text{ext}} + \mathscr{M}, \tag{22}$$

where $\mathscr{P}_{\text{ext}}$ is the external power. In addition to the classical terms of macroscopic forces, we consider non-classical terms contributing to the energy balance. This includes power expenditures of the microforces in $\mathscr{P}_{\text{ext}}$ along with energy flux due to the species diffusion (i.e., fluxes and sources). In (22), $\mathscr{M}$ is the (free-)energy carried into $\mathscr{R}_t$ by mass (species) transport (see, e.g., [62, 66, 98]). As $\mathbf{J}_a$ and S_a carry with them a flux and supply of energy, respectively, characterized by the chemical potential μ_a, we write

$$\mathscr{M} = \sum_{\alpha} \left(- \int_{\partial \mathscr{R}_t} \mu_{\alpha} \mathbf{J}_{\alpha} \cdot \mathbf{n} \, \mathrm{d}A + \int_{\mathscr{R}_t} \mu_{\alpha} S_{\alpha} \, \mathrm{d}V \right). \tag{23}$$

The chemical potential μ_α of species α is a quantity defined as the rate of change of free energy with respect to the change in the particle number of the species that are added or removed from the thermodynamic system. The magnitude of the chemical potential is independent of the size of the system, but it does include phenomena affecting diffusion; e.g., the strain energy gradient, electric field, and temperature gradient. Thus, in (23), μ_α characterizes the flux and supply of energy to the system and needs to be considered in the energy balance relation.

From the mass balance relation (16), along with the divergence theorem,

$$\begin{aligned}\int_{\partial\mathscr{R}_t}\mu_\alpha\mathbf{J}_\alpha\cdot\mathbf{n}\,\mathrm{d}A &= \int_{\mathscr{R}_t}(\mu_\alpha\nabla\cdot\mathbf{J}_\alpha+\nabla\mu_\alpha)\,\mathrm{d}V\\ &= -\left(\mu_\alpha\frac{d^\alpha\rho_\alpha\phi_\alpha}{dt}-\mathbf{J}_\alpha\cdot\nabla\mu_\alpha-\mu_\alpha S_\alpha\right)\mathrm{d}V,\end{aligned}$$

one can write,

$$\mathscr{M}=\sum_\alpha\int_{\mathscr{R}_t}\left(\mu_\alpha\frac{d^\alpha\rho_\alpha\phi_\alpha}{dt}-\mathbf{J}_\alpha\cdot\nabla\mu_\alpha\right)\mathrm{d}V\,.$$

Consequently, (22) can be written as,

$$\begin{aligned}\frac{d}{dt}\int_{\mathscr{R}_t}\rho\varepsilon\,\mathrm{d}V \coloneqq &\sum_\alpha\int_{\mathscr{R}_t}\left(\mathbf{T}_\alpha:\mathbf{L}_\alpha+\tau_\alpha\frac{d^\alpha\phi_\alpha}{dt}\right)\mathrm{d}V+\sum_\alpha\int_{\partial\mathscr{R}_t}(\boldsymbol{\xi}_\alpha\cdot\mathbf{n})\frac{d^\alpha\phi_\alpha}{dt}\,\mathrm{d}A\\ &+\sum_\alpha\int_{\mathscr{R}_t}\left(\mu_\alpha\frac{d^\alpha\rho_\alpha\phi_\alpha}{dt}-\mathbf{J}_\alpha\cdot\nabla\mu_\alpha\right)\mathrm{d}V\,.\end{aligned}\tag{24}$$

From the symmetry of the Cauchy stress in (13), the term $\mathbf{T}_\alpha:\mathbf{L}_\alpha$ can be replaced by $\mathbf{T}_\alpha:\mathbf{D}_\alpha$. Moreover, applying the divergence theorem again yields,

$$\int_{\partial\mathscr{R}_t}(\boldsymbol{\xi}_\alpha\cdot\mathbf{n})\frac{d^\alpha\phi_\alpha}{dt}dA=\int_{\mathscr{R}_t}\boldsymbol{\xi}_\alpha\nabla\left(\frac{d^\alpha\phi_\alpha}{dt}\right)dV+\int_{\mathscr{R}_t}(\nabla\cdot\boldsymbol{\xi}_\alpha)\frac{d^\alpha\phi_\alpha}{dt}dV,$$

along with

$$\nabla\cdot\boldsymbol{\xi}_\alpha\frac{d^\alpha\phi_\alpha}{dt}+\tau_\alpha\frac{d^\alpha\phi_\alpha}{dt}=-\tau_\alpha\frac{d^\alpha\phi_\alpha}{dt}.$$

Following (15), the relation for the *local energy balance* is derived as,

$$\rho\frac{d\varepsilon}{dt} = \sum_{\alpha}\left(\mathbf{T}_{\alpha}:\mathbf{D}_{\alpha} - \pi_{\alpha}\frac{d^{\alpha}\phi_{\alpha}}{dt} + \boldsymbol{\xi}_{\alpha}\cdot\nabla\left(\frac{d^{\alpha}\phi_{\alpha}}{dt}\right)\right) + \sum_{\alpha}\left(\mu_{\alpha}\frac{d^{\alpha}\rho_{\alpha}\phi_{\alpha}}{dt} - \mathbf{J}_{\alpha}\cdot\nabla\mu_{\alpha}\right). \tag{25}$$

It is worth mentioning that both $\mathbf{b}_{\alpha}$ and $\boldsymbol{\pi}_{\alpha}$ are internal forces in $\mathscr{R}_t$ at the macroscopic and microscopic length scales respectively. While $\mathbf{b}_{\alpha}$ and $\boldsymbol{\pi}_{\alpha}$ exist in the force balances (12) and (15), they are not present in the working terms of the energy equation(24). Moreover, the balance equation (22) for the mixture is transferred into individual constituents, in which the local and global balances are related according to

$$\rho\frac{d\varepsilon}{dt} = \sum_{\alpha}\rho_{\alpha}\phi_{\alpha}\frac{d^{\alpha}\varepsilon_{\alpha}}{dt}. \tag{26}$$

2.5.2 The Second Law: Entropy Production Inequality—The second law of thermodynamics (entropy principle) is used here for imposing restrictions on constitutive equations. In mixture theory, while the implementation of such constraints for every individual species is possible and restrictive, its satisfaction for all constituents is a necessary and sufficient condition for the presence of dissipative processes within the mixture [37, 38]. It should also be noted that the entropy inequality has to be manipulated to include fundamental and special physical properties of the system under study. Depending on the behavior of the body, the supplementary constraints might be taken into consideration at the local (constituent) level and/or applied globally to the full mixture[4]. Moreover, this inequality is a necessary constraint on constitutive equations. There is not a unique way to fulfill this inequality, and many choices that satisfy the inequality may lead to simulations that do not accurately reflect the physical phenomena.

The entropy production inequality requires that the free energy increases at a rate not greater than the rate at which work is performed. The net entropy production per unit time, is given by

$$\mathscr{N} = \frac{d}{dt}\int_{\mathscr{R}_t}\eta dV \geq 0, \tag{27}$$

where η is the specific entropy of the mixture and (27) is often referred to as the Clausius-Duhem inequality [69, 70]. The entropy density of the mixture can be written as a sum of the specific entropy of individual constituents as

[4]In the continuum theory of mixtures, one might need to impose additional conditions (e.g., incompressibility or rigidity of any of the species or a saturation condition), to treat the mixture as smeared continua. These conditions can be provided by Lagrange multipliers in postulating the entropy production inequality, according to the thermodynamic theory of constraint developed by Gurtin and Guidugli [67]. Alternatively, these condition can be considered as an additional energy term in the equation for energy balance and corresponding force balance [20, 126].

$$\rho\eta = \sum_{\alpha} \rho_\alpha \phi_\alpha \eta_\alpha \,. \tag{28}$$

We continue with the derivation of the Clausius-Duhem inequality by defining the Helmholtz (specific) free-energy of the mixture as,

$$\psi(\mathbf{x}, t) = \varepsilon(\mathbf{x}, t) - \theta(\mathbf{x}, t)\, \eta(\mathbf{x}, t) \,. \tag{29}$$

The free-energy per unit volume is,

$$\Psi(\mathbf{x}, t) = \rho\psi(\mathbf{x}, t), \tag{30}$$

with the free energy for every individual species (e.g., [120]) given as,

$$\Psi_\alpha = \rho_\alpha \phi_\alpha \psi_\alpha \,.$$

Taking the time derivative of free-energy and substituting (25) into (29) along with (30), yields the local free-energy imbalance for fixed temperature $\theta = \theta_0$[5],

$$\begin{aligned} &-\frac{d\Psi}{dt} + \sum_{\alpha} \left(\mathbf{T}_\alpha : \mathbf{D}_\alpha - \tau_\alpha \frac{d^\phi \phi_\alpha}{dt} + \boldsymbol{\xi}_\alpha \cdot \nabla \left(\frac{d^\alpha \phi_\alpha}{dt} \right) \right) \\ &+ \sum_{\alpha} \left(\mu_\alpha \frac{d^\alpha \rho_\alpha \phi_\alpha}{dt} - \mathbf{J}_\alpha \cdot \nabla \mu_\alpha \right) \geq 0 \,. \end{aligned} \tag{31}$$

The invariance properties discussed in [43] lead to all quantities in (31) being invariant under a change in frame.

The force balance equations (12) and (15), mass balance (17), along with first and second laws of thermodynamics (25) and (31) describe balance laws for a constituent α in a mixture of N constituents. The requirements that these balance laws must be consistent with those for the mixture as a whole imposes constraints depicted in (21). This system is closed by adding suitable constitutive equations and describing the physical and biological processes that might take place in the mixture.

2.6 Coleman-Noll Procedure

The balance laws for mass and momentum as well as the first and second laws of thermodynamics are presumed to hold for all bodies. It is necessary to prescribe constitutive equations for a particular material, and the processes that bodies comprised of the given material may undergo. Within rational continuum mechanics, the Coleman-Noll procedure [34] is established to derive requirements for constitutive equations. According to Ziegler

[5]It should be noted that throughout this formulation we work with the free energy per unit volume of the mixture Ψ. Alternative derivations can be conducted using Helmholtz free-energy per unit mass ψ or considering the free energy for every individual species; see, e.g., [120].

[172], continuum mechanics allows one to establish constitutive relations, deduced from free energy and dissipation functions characterizing reversible and irreversible processes, respectively. This leads to the decomposition of the thermodynamic conjugate forces into energetic and dissipative counterparts. The energetic forces are entirely determined by the specific free energy while the dissipative forces are determined from the dissipative function [170, 171]. Guided by the inequality in (31), it is assumed that the Cauchy stress tensor for each species admits the decomposition into energetic and dissipative components,

$$\mathbf{T}_\alpha = \mathbf{T}_\alpha^{en} + \mathbf{T}_\alpha^{dis}, \tag{32}$$

while other thermodynamical conjugate forces are identified as completely energetic or dissipative in nature. This choice is made based upon our current knowledge about the physical and biological events that contribute to the tumor growth process. In general, other conjugate forces can be decomposed as in (32) where additional phenomena are identified that contribute to energy storage and dissipation[6].

To derive the relation between thermodynamic forces. The Helmholtz free energy, Ψ, and dissipative potentials, $\mathscr{D}$, we initially consider a general form of free energy considering the contribution of μ and $\nabla\mu$, and assuming a system far from equilibrium (μ is not given).[7],

$$\begin{aligned}\Psi = \Psi(&\mathbf{F}_1, \cdots, \mathbf{F}_N, \rho_1, \cdots, \rho_N, \phi_1, \cdots, \phi_N,\\ &\nabla\phi_1, \cdots, \nabla\phi_N, \mu_1, \cdots, \mu_N, \nabla\mu_1, \cdots, \nabla\mu_N).\end{aligned} \tag{33}$$

The time derivation of Ψ (using the chain rule) results in,

$$\begin{aligned}\frac{d\Psi}{dt} = \sum_\alpha \Bigg(&\frac{\partial\Psi}{\partial(\mathbf{C}_\alpha, \mathbf{F}_\alpha)} : \mathbf{D}_\alpha + \frac{\partial\Psi}{\partial\rho_\alpha}\frac{d^\alpha\rho_\alpha}{dt} + \frac{\partial\Psi}{\partial\phi_\alpha}\frac{d^\alpha\phi_\alpha}{dt} + \frac{\partial\Psi}{\partial(\nabla\phi_\alpha)}\frac{d^\alpha(\nabla\phi_\alpha)}{dt}\\ &+ \frac{\partial\Psi}{\partial\mu_\alpha}\frac{d^\alpha\mu_\alpha}{dt} + \frac{\partial\Psi}{\partial(\nabla\mu_\alpha)}\frac{d^\alpha(\nabla\mu_\alpha)}{dt}\Bigg),\end{aligned} \tag{34}$$

Where

$$\frac{\partial\Psi}{\partial(\mathbf{C}_\alpha, \mathbf{F}_\alpha)} : \mathbf{D}_\alpha = \begin{cases} 2\mathbf{F}_\alpha^T \dfrac{\partial\Psi}{\partial\mathbf{C}_\alpha}\mathbf{F}_\alpha : \mathbf{D}_\alpha, & 1 < \alpha \le M,\\ \dfrac{\partial\Psi}{\partial\mathbf{F}_\alpha}\mathbf{F}_\alpha^T : \mathbf{D}_\alpha, & M < \alpha \le N. \end{cases} \tag{35}$$

Making use of the gradient of material time derivatives,

[6] An example can be found in the generalized Cahn-Hilliard equation derived by Gurtin [62] in which both the microstress $\boldsymbol{\xi}$ and microforce $\boldsymbol{\pi}$ are decomposed into energetic and dissipative counterparts.

[7] For a multiphase system, a condition for equilibrium is that the chemical potential of each component must be the same in all phases. This follows from the total change in free energy being zero at equilibrium; see, e.g., [145].

$$\nabla\left(\frac{d^{\alpha}\phi_{\alpha}}{dt}\right)=\frac{d^{\alpha}}{dt}(\nabla\phi_{\alpha})+\nabla\cdot\mathbf{v}_{\alpha}\cdot\nabla\phi_{\alpha},$$

along with substituting (34) into the free energy imbalance (31) and grouping terms together, we find the following inequality

$$\begin{aligned}\sum_{\alpha}\Bigg\{&\left(\mathbf{T}_{\alpha}^{en}-\frac{\partial\Psi}{\partial(\mathbf{C}_{\alpha},\mathbf{F}_{\alpha})}+\xi_{\alpha}\otimes\nabla\phi_{\alpha}\right):\mathbf{D}_{\alpha}+\left(-\pi_{\alpha}+\rho_{\alpha}\mu_{\alpha}-\frac{\partial\Psi}{\partial\phi_{\alpha}}\right)\frac{d^{\alpha}\phi_{\alpha}}{dt}\\&+\left(\xi_{\alpha}-\frac{\partial\Psi}{\partial(\nabla\phi_{\alpha})}\right)\frac{d^{\alpha}(\nabla\phi_{\alpha})}{dt}-\frac{\partial\Psi}{\partial\mu_{\alpha}}\frac{\partial\mu_{\alpha}}{dt}-\frac{\partial\Psi}{\partial(\nabla\mu_{\alpha})}\frac{d^{\alpha}(\nabla\mu_{\alpha})}{dt}+\mu_{\alpha}\rho_{\alpha}\frac{\partial\Psi}{\partial\rho_{\alpha}}\frac{d^{\alpha}\rho_{\alpha}}{dt}\\&+\ \mathbf{T}_{\alpha}^{dis}:\mathbf{D}_{\alpha}-\nabla\mu_{\alpha}\cdot\mathbf{J}_{\alpha}\Bigg\}\geq 0\,.\end{aligned}\tag{36}$$

The classical Coleman-Noll argument asserts that, in order that the inequality (36) hold, the coefficient of quantities such as $\mathbf{D}_{\alpha}$, $d^{\alpha}\phi_{\alpha}/dt$, etc. must vanish as these terms can assume arbitrary large negative values. Thus, the fact that the time derivatives of the variables are arbitrary, results in the following choices being sufficient to ensure the free energy inequality,

$$\xi_{\alpha}=\frac{\partial\Psi}{\partial(\nabla\phi_{\alpha})},\tag{37}$$

$$\mathbf{T}_{\alpha}^{en}=\frac{\partial\Psi}{\partial(\mathbf{C}_{\alpha},\mathbf{F}_{\alpha})}-\xi_{\alpha}\otimes\nabla\phi_{\alpha},\tag{38}$$

$$\pi_{\alpha}\ =\ \rho_{\alpha}\mu_{\alpha}-\frac{\partial\Psi}{\partial\phi_{\alpha}}\,.\tag{39}$$

The above relations defines the energetic part of the thermodynamic forces. Using the microforce balance (15), one can derive a relation for the chemical potential such as

$$\rho_{\alpha}\mu_{\alpha}=\frac{\partial\Psi}{\partial\phi_{\alpha}}-\nabla\cdot\xi_{\alpha}-\tau_{\alpha}\tag{40}$$

which can be simplified further by replacing $\boldsymbol{\xi}_{\alpha}$ from (37).

By a similar Coleman-Noll argument we have,

$$\frac{\partial\Psi}{\partial\rho_{\alpha}}=0,\ \ \frac{\partial\Psi}{\partial\mu_{\alpha}}=0,\ \ \frac{\partial\Psi}{\partial(\nabla\mu_{\alpha})}=\mathbf{0},\tag{41}$$

suggesting that the thermodynamic process is admissible if and only if the Helmholtz free energy density is independent of ρ_{α}, μ_{α} and $\nabla\mu_{\alpha}$. Thus, the free energy takes a simpler form[8],

$$\Psi = \Psi\left(\mathbf{F}_1, \cdots, \mathbf{F}_N, \phi_1, \cdots, \phi_N, \nabla\phi_1, \cdots, \nabla\phi_N\right). \tag{42}$$

Not all power expended on a spatial region can be transformed into changes in the free energy, and part of the power goes into dissipation. Thus, the remaining terms in the inequality (36), after considering (37)-(39), are the rate of dissipation potential,

$$\mathscr{D} = \sum_{\alpha}\left\{\mathbf{T}_{\alpha}^{dis} : \mathbf{D}_{\alpha} - \nabla\mu_{\alpha}\cdot\mathbf{J}_{\alpha}\right\} \geq 0.$$

The definition of the dissipative thermodynamic forces can then be obtained from the complementary part of dissipation potential as,

$$\mathbf{T}_{\alpha}^{dis} = \frac{\partial\mathscr{D}}{\partial\mathbf{D}_{\alpha}}, \tag{43}$$

$$\mathbf{J}_{\alpha} = \frac{\partial\mathscr{D}}{\partial\nabla\mu_{\alpha}}, \tag{44}$$

Where

$$\mathscr{D} = \mathscr{D}\left(\mathbf{D}_1, \cdots, \mathbf{D}_N, \phi_1, \cdots, \phi_N, \nabla\phi_1, \cdots, \nabla\phi_N, \nabla\mu_1, \cdots, \nabla\mu_N\right). \tag{45}$$

2.7 Constitutive Relations for the Admissible Potentials

The continuum theory presented here attempts to provide a general framework for addressing many of the complex biological phenomena that take place in cancer. This consists of multiple interactions among various constituents. In this regard, it is considered that the N-species mixture consists of M solid constituents undergoing both hyper-elastic deformation and biological growth and $N-M$ viscous compressible fluid constituents. The constitutive relations are defined by proposing two primary potentials, Helmholtz free energy, and the rate of dissipation.

2.7.1 Helmholtz Free Energy—We postulate the following general definition of the free energy of the mixture,

$$\Psi = \Psi^{\text{els}} + \Psi^{\text{chm}} + \Psi^{\text{int}} + \Psi^{\text{taxis}}, \tag{46}$$

where Ψ^{els} denotes elastic energy for solid species and Ψ^{chm} and Ψ^{int} represents (bio-)chemical energy and interface counterparts, respectively, normally employed in phase-field models. The free energy functional also includes the energy due to taxis-inducing chemical and molecular species, Ψ^{taxis}; see, e.g., [1, 35, 96].

[8]One can initially assume more general forms of free energy considering contributions of other quantities; e.g., time derivative of the volume fraction [98-100]. The Coleman-Noll procedure then results in a corresponding reduction in the forms of the Helmholtz free energy.

Hereafter, we assume the fluid constituents of the mixture are compressible, thus

$$\frac{\partial \Psi^{\text{els}}}{\partial \mathbf{F}_\alpha}\mathbf{F}_\alpha^T = -p_\alpha \mathbf{I}, \qquad M < \alpha \leq N,$$

where p_α is the classical equilibrium pressure,

$$-p_\alpha = \hat{\rho}_\alpha^2 \frac{\partial \psi_\alpha}{\partial \hat{\rho}_\alpha}, \qquad M < \alpha \leq N, \tag{47}$$

where $\hat{\rho}_I$ is the mass density of constituent (4), and the thermodynamic pressure is represented as the derivative of free energy per unit mass for each fluid constituent. Moreover, the solid species are considered to be isotropic hyperelastic. In a hyperelastic body, the Piola-Kirchhoff stress is the derivative of a scalar function W called strain energy density. Therefore, the second Piola-Kirchhoff stress is given by,

$$\mathbf{S}_\alpha = \det \mathbf{F}_\alpha \mathbf{F}_\alpha^{-1} \mathbf{T}_\alpha \mathbf{F}_\alpha^{-T} = \frac{\partial W_\alpha}{\partial \mathbf{C}_\alpha}, \qquad 1 < \alpha \leq M, \tag{48}$$

where $\mathbf{C}_\alpha = \mathbf{F}_\alpha^T \mathbf{F}_\alpha$ is the right Cauchy-Green deformation tensor and $W_\alpha = W_\alpha(\mathbf{C}_\alpha, \boldsymbol{\phi}_\alpha)$ represents the strain energy function for the α-th solid constituent[9]. The strain energy density and elastic free energy are related through the mass density of a constituent in the reference configuration, $W_\alpha = \rho_\alpha^0 \phi_\alpha^0 \psi_\alpha^{\text{els}}$.

An important class of diffuse-interface or phase-field models of Cahn-Hilliard type are characterized by a Helmholtz free energy that consists of a double-well potential function for $\Psi^{\text{chm}} = \Psi^{\text{chm}}(\boldsymbol{\phi}_1, \cdots, \boldsymbol{\phi}_N)$ called a "coarse-grain" free energy, and an interfacial energy of the form,

$$\Psi^{\text{int}} = \Psi^{\text{int}}(\nabla \boldsymbol{\phi}_1, \cdots, \nabla \boldsymbol{\phi}_N) = \sum_\alpha \frac{\epsilon_\alpha}{2} \mid \nabla \boldsymbol{\phi}_\alpha \mid^2, \tag{49}$$

where ϵ_α (sometime referred to as the Landau-Ginzburg constants) characterizes the interface thickness. The interfacial energy (49) models longer-range interactions among the components by representing the effects of large gradients in concentrations that occur at interface regions between different constituents.

Following [35, 164], the effect of energy due to taxis-inducing chemical and molecular species is included in the free energy by,

$$\Psi^{\text{taxis}} = (\boldsymbol{\phi}_1, \cdots, \boldsymbol{\phi}_N) = \sum_\alpha \boldsymbol{\phi}_\alpha \sum_{\beta=1}^{L} \eta_{\alpha\beta} c_\beta, \tag{50}$$

[9]The kinematic of biological growth of the solid species along with the constitutive laws are discussed in the following section.

where c_β, $1 \le \beta \le L$, are the concentrations of chemical factors that may induce taxis (e.g., various sources of nutrient) and $\eta_{a\beta}$ is the taxis coefficient. In particular, (50) accounts for the reaction between concentrations of various vital nutrients in the mixture (such as oxygen or glucose) and the constituent a. This relation enables describing complex invasive behavior of a tumor observed in *in vivo.* Here, taxis refers to directional migration toward particular chemical or molecular species (i.e., chemotaxis) gradients or toward adhesion site gradients (i.e., haptotaxis). In a chemotaxis scenario, cells migrate in the direction of increased nutrient concentration [71]. The movement of the nutrient towards the tumor can be seen as active transport of the nutrient [54]. Garcke *et al* [54] studied the effects of chemotaxis and active transport on the tumor growth. Through numerical experiments, they verified the jump on the nutrient concentration at the tumor interface due to active transport. In vascular models of tumor growth (e.g., [9, 96]), the chemotactic term accounts for the endothelial cells moving up the concentration gradient of vascular endothelial growth factor (VEGF). VEGF is a pro-angiogenic factor released by tumor cells in an effort to recruit new vasculature to support further tumor growth [128].

2.7.2 Rate of Dissipation Potential—As discussed in section 2.6, energetic-dissipative decomposition of the thermodynamic conjugate forces results in the development of an energy dissipation rate. Here the dissipation energy potential can be considered as the summation of dissipations due to viscosity $\mathscr{D}^{\text{vis}}$ and diffusion $\mathscr{D}^{\text{diff}}$,

$$\mathscr{D} = \mathscr{D}^{\text{vis}} + \mathscr{D}^{\text{diff}} \ge 0 .$$

For hyperelastic solid constituents,

$$\mathscr{D}^{\text{vis}}(\mathbf{D}_1, \cdots, \mathbf{D}_M, \phi_1, \cdots, \phi_M) = 0,$$

where $\mathbf{D}_a$ is defined in (9) and we assume the internal viscosity of fluid species can be described by a dissipation potential as a general isotropic, second-order tensor function of deformation rate,

$$\mathscr{D}^{\text{vis}}(\mathbf{D}_{M+1}, \cdots, \mathbf{D}_N, \phi_{M+1}, \cdots, \phi_N) = \sum_\alpha \frac{1}{2} A_\alpha \mid \mathbf{D}_\alpha \mid^2 , \quad M < \alpha \le N, \tag{51}$$

where $A_a(\phi_a)$ is the shear viscosity of fluid species. The above relation results in a dissipative counterpart of the Cauchy stress,

$$\mathbf{T}_\alpha^{dis} = A_\alpha \mathbf{D}_\alpha, \quad M < \alpha \le N . \tag{52}$$

Cahn-Hilliard type equations are considered in this formulation for characterizing the energy dissipation due to diffusion,

$$\mathscr{D}^{\text{diff}}(\mathbf{D}_1, \cdots, \mathbf{D}_N, \phi_1, \cdots, \phi_N, \mu_1, \cdots, \mu_N) = \sum_\alpha \nabla \mu_\alpha \cdot \mathbf{M}_\alpha \cdot \nabla \mu_\alpha \tag{53}$$

where μ_a is the chemical potential and $\mathbf{M}_a = \mathbf{M}_a(\mathbf{C}_a, \phi_a)$ is the positive semi-definite mobility tensor. Using the frame-indifference principle discussed in [43], it can be shown that $\mathbf{M}_a$ is symmetric and invariant under a change in frame.

2.7.3 Energetic and Dissipative Forces—From the functional forms of Ψ and $\mathscr{D}$, one can derive relations for the thermodynamic forces. From (37), the energetic micro-stress $\boldsymbol{\xi}_a$ has the form

$$\xi_\alpha = \epsilon_\alpha \nabla \phi_\alpha \,. \tag{54}$$

Using (38) and (43), the Cauchy stress for solid and fluid constituents can be derived as

$$\mathbf{T}_\alpha = \mathbf{T}_\alpha^{en} + \mathbf{T}_\alpha^{dis} = \begin{cases} \frac{2}{\det \mathbf{F}_\alpha} \mathbf{F}_\alpha \mathbf{S}_\alpha \mathbf{F}_\alpha^T - \epsilon_\alpha \nabla \phi_\alpha \otimes \nabla \phi_\alpha & , \quad 1 < \alpha \leq M \\ p_\alpha \mathbf{I} + A_\alpha \mathbf{D}_\alpha - \epsilon_\alpha \nabla \phi_\alpha \otimes \nabla \phi_\alpha & , \quad M < \alpha \leq N \end{cases} \tag{55}$$

The $\boldsymbol{\xi}_a$ enters in species microforce balance (recall (14) and (15)) as a flux and divergence term. This suggests that $\boldsymbol{\xi}_a$ is an stress-type quantity and associated with the interaction forces at the interface of the constituents. From (54), one can argue that the microstress $\boldsymbol{\xi}_a$ accounts for cell adhesion due to volume fraction changes at the interface of each constituent. In contrary to (for example) the chemotaxis phenomenon which can be addressed with a local model, cell adhesion is intrinsically a non-local process [141]. The nonlocality arises because the cellular adhesion forms a biological interaction between cells and their surroundings such that cells contribute adhesion molecules at its position as well as its neighboring region [27]. Following a phase-field approach and acknowledging the existence of microscopic force balances, results in automatic incorporation of cell adhesion in the current model, a phenomenon that is challenging to address using local continuum models [15, 141]. The term ϵ_a is the interaction parameter and represents the thickness of the interface (i.e., how sharp is the interface between the phases). In biological processes involved in tumor growth, this term is directly related to the cell-cell adhesion [36, 104]. Sharp interfaces (i.e., ϵ_a close to zero with a indicating tumor constituent) can model cells with high adhesion such as epithelial tumors [156] and increasing the value of interface thickness enables mimicking the behavior of cells with low adhesion and higher motility as glioblastoma and stromal cells [84, 104, 133]. This relation suggests that stronger cell-cell adhesion results in sharper interfaces and more compact morphology. The first term in the Cauchy stress of solid constituents in (55) reflects the hyperelastic deformation with growth. However, the microforce balance of (15) results in another term in the Cauchy stress; i.e., $\epsilon_a \nabla \phi_a \otimes \nabla \phi_a$. In biological processes, this term mimics surface tension-like cell-adhesion forces in the Cauchy stress and exists in the absence of elastic deformation (see [43] for the evolution of this counterpart of the Cauchy stress).

Another dissipative thermodynamic force is the mass flux that can be derived from (44) and (53) as,

$$\mathbf{J}_\alpha = -\mathbf{M}_\alpha \cdot \nabla \mu_\alpha . \tag{56}$$

Assuming (56) holds, the equation describing the evolution of species content (recall (17)) becomes,

$$\frac{\partial \rho_\alpha \phi_\alpha}{\partial t} + \nabla \cdot (\rho_\alpha \phi_\alpha \mathbf{v}_\alpha) = S_\alpha - \nabla \cdot (\mathbf{M}_\alpha \cdot \nabla \mu_\alpha) . \tag{57}$$

Making use of (39), the chemical potential can be derived as,

$$\rho_\alpha \mu_\alpha = \frac{\partial \Psi^{\text{els}}}{\partial \phi_\alpha} + \frac{\partial \Psi^{\text{chm}}}{\partial \phi_\alpha} + \sum_{\beta=1}^{L} \eta_{\alpha\beta} c_\beta - \epsilon_\alpha \Delta \phi_\alpha - \tau_\alpha, \tag{58}$$

where Δ denotes the spatial Laplacian operator (i.e., $\Delta = \nabla \cdot \nabla$). Relation (58) indicates the dependency of μ_α on volume fractions[10].

Equation (57) represents a system of N fourth-order, parabolic partial differential equations of the Cahn-Hilliard type. These equations along with the macro-force balance (12), together with the appropriate boundary and initial conditions, characterize a general coupled phase-field and elastic deformation, continuum mixture model of a complex media consisting of multiple solid and fluid species. The constituents can be compressible, the fluid species are Newtonian, the solid constituents are isotropic hyperelastic, and the effects of diffusion of chemical or biological constituents due to chemo- or bio-taxis as well as surface effects due to gradients in concentrations are included.

To apply such general models in a meaningful manner to simulate tumor growth, several specific details are needed. These include specific forms of the constitutive equations for each constituent along with the inclusion of growth effects due to mass exchange and deformation. These are discussed in detail in the next section.

3 A Four-Constituent Phase-Field Model of Tumor Growth

In this section, the general multi-species theory described in section 2 is adapted to simulate the significant features of the growth of tumors in a microenvironment. We derive a coupled formulation for diffusion and large elastic deformation of avascular tumor based on a hybrid 10-constituent phase-field model proposed by Lima et al. [94, 96]. The tumor volume fraction ϕ_T accounts for proliferative, hypoxic, and necrotic cells and ϕ_σ indicates the nutrient volume fraction so-called nutrient-rich extracellular water according to [35]. In particular, we consider a mixture consists of four constituents by considering two complementary species, ϕ_C, and $\phi_{\sigma 0}$. ϕ_C represents the normal (healthy) cells, and it is complimentary to tumor volume fraction ϕ_T, while $\phi_{\sigma 0}$ is the complimentary constituent to

[10]While most of the phase transformation theories of the type considered here are consistent with the dependency of the chemical potential on volume fractions, in some special situations the chemical potential cannot be expressed as a function of volume fraction [50, 51].

the nutrient volume fraction, hereon called nutrient-poor extracellular water. Then the saturation condition of the mixture $\phi_T + \phi_C + \phi_\sigma + \phi_{\sigma 0}$, is enforced by rescaling the volume fractions. The solid, $s = \phi_T + \phi_C$, and fluid, $w = \phi_\sigma + \phi_{\sigma 0}$ are assumed to vary from 0 to 1 depending on a constant C by defining $s = C$ and $w = 1 - C$. This rescaling normalizes the values of ϕ_T and ϕ_σ to take on values between 0 and 1 and the volume fraction of the healthy computed as $\phi_C = 1 - \phi_T$.

The tumor cells (proliferative, hypoxic, and necrotic) have similar adhesive properties and they prefer to adhere to one another [35, 97], causing a segregation from healthy cells. This behavior of separation among phases, typical of binary Cahn-Hilliard systems, is modeled by a double-well potential and a capillary interfacial energy. The presence of a nutrient-rich volume fraction in the mixture contributes to an increase of the system energy through a quadratic term and interacts chemotactically with tumor cells, yielding a directional movement towards the nutrient supply [96, 164]. These assumptions yield the following chemical and interface components of the Helmholtz free energy of the system:

$$\Psi^{\text{chm}}(\phi_T, \phi_\sigma) = \kappa \phi_T^2 (1 - \phi_T)^2 + \frac{1}{2\delta_\sigma} \phi_\sigma^2, \tag{59}$$

$$\Psi^{\text{int}}(\nabla \phi_T, \nabla \phi_\sigma) = \frac{\epsilon_T^2}{2} \mid \nabla \phi_T \mid^2, \tag{60}$$

where the coefficient $\kappa > 0$ in the quadratic double-well function is an energy scale giving rise to a well-delineated phase separation of the tumor and the host tissues. In (59), δ_σ is a coefficient that controls the increase of energy due to nutrient volume fraction. The interfacial surface energy due to spatial gradient of the tumor volume fraction is defined through an interaction length parameter ϵ_T. In particular, ϵ_T controls the interface among tumor cells and other constituents. The effect of energy due to taxis-inducing chemical and molecular species is addressed through,

$$\Psi^{\text{taxis}}(\phi_T, \phi_\sigma) = -\chi_0 \phi_T \phi_\sigma, \tag{61}$$

where $\chi_0 > 0$ is a constant governing the relative strength of the interaction between tumor cells and nutrient.

We take into account a Cahn-Hilliard type energy dissipation due to diffusion, such as

$$\mathscr{D}^{\text{diff}} = \nabla \mu_T \cdot \mathbf{M}_T \cdot \nabla \mu_T + \nabla \mu_\sigma \cdot \mathbf{M}_\sigma \cdot \nabla \mu_\sigma . \tag{62}$$

The coupling effect of deformation on the tumor mass transfer results in the dependency of tumor mobility and mass exchange to a measure of deformation. Modeling this dependency is discussed in the following section. Finally, the energy dissipation due to viscosity is considered to be,

$$\mathscr{D}^{\text{vis}} = \frac{1}{2} A_\sigma \mid \mathbf{D}_\sigma \mid^2 , \tag{63}$$

where A_σ is extracellular water viscosity coefficient [132].

3.1 Kinematics of Hyperelastic, Growing Solid Tumor

The mechanical stresses of a solid tumor have fundamental implications for both its growth [72] and response to treatment [160]. For example, it has been shown that compression of cancer cells reduces their proliferation rate, induces apoptosis, and enhances their invasive and metastatic potential. Thus, tumors that manifest higher stress levels may have lower growth rates and a higher tendency to metastasize [26, 30, 40, 78, 79, 85, 91, 157]. Moreover, the force applied by the surrounding tissue during the growth of a tumor can alter both tumor expansion and shape [72, 74, 159, 160, 162]. Here we consider two mechanisms participating in the mechanical behavior of a tumor: *the externally applied stress* due to mechanical interactions among the solid components of the growing tumor and the surrounding tissue, and *the growth-induced stress* due to proliferating cancer cells

We consider the kinematics of growth such that the total deformation gradient result from a geometrically necessary elastic deformation associated with mass growth, along with a deformation due to an externally applied stress. Consequently, the deformation gradient of the tumor, $\mathbf{F}_T$, accepts the following decomposition (see, e.g., [57]),

$$\mathbf{F}_T = \mathbf{F}_T^S \mathbf{F}_T^G, \tag{64}$$

where $\mathbf{F}_T^G$ is the growth deformation gradient tensor, that acting alone leads to incompatible deformation [144] leading to residual stresses developments. $\mathbf{F}_T^S$ is the elastic component of the deformation gradient tensor that accounts for the elastic deformation required to ensure compatibility (resulting in the internal growth-induced stress) as well as the deformation due to external stress such as surrounding tissue confinements [57]. The multiplicative decomposition (64) is based on introducing an intermediate unstressed configuration by elastic distressing of the current configuration $\mathscr{B}_t$ to zero stress. Assuming the elasticity parameters are independent of tumor volume fraction, one can write

$$\frac{\partial \Psi^{\text{els}}}{\partial \mathbf{F}_T} = \frac{\partial \Psi^{\text{els}}}{\partial \mathbf{F}_T^S} : \frac{\partial \mathbf{F}_T^S}{\partial \mathbf{F}_T}, \tag{65}$$

where

$$\frac{\partial \mathbf{F}_T^S}{\partial \mathbf{F}_T} = \frac{\partial \mathbf{F}_T (\mathbf{F}^G)^{-1}}{\partial \mathbf{F}_T} = \mathbf{I} \otimes (\mathbf{F}^G)^{-1} . \tag{66}$$

We consider a compressible Neo-Hookean material for the tumor material[11] that is a commonly used constitutive model for the elastic response of soft tissue [53, 105, 157]. The strain energy function is,

$$W = \frac{G_T}{2}\left((J_T^S)^{-\frac{2}{3}} I_{C_1}^S - 3\right) + \frac{K_T}{2}(J_T^S - 1)^2, \tag{67}$$

where G_T and K_T are shear and bulk modulus, respectively, and I_{C1}^S is the first invariant of the right Cauchy-Green deformation tensor defined as,

$$I_{C_1}^S = \mathrm{tr}(\mathbf{C}_T^S), \tag{68}$$

where $\mathbf{C}_T^S = (\mathbf{F}_T^S)^T \mathbf{F}_T^S$. In (67), J_T^S is a volume change measure,

$$J_T^S = \sqrt{\det(\mathbf{C}_T^S)} = \det(\mathbf{F}_T^S)\,. \tag{69}$$

From (55) and the specific form of strain energy (67), a relation for the Cauchy stress is obtained as,

$$\mathbf{T}_T = \left(\frac{G_T}{J_T^{S\,5/3}}\left(\mathbf{B}_T^S - \frac{1}{3} tr(\mathbf{B}_T^S)\mathbf{I}\right) + K_T(J_T^S - 1)\mathbf{I}\right)(\mathbf{F}_T^G)^{-T} - \epsilon_T \nabla\phi_T \otimes \nabla\phi_T, \tag{70}$$

where $\mathbf{B}_T^S = \mathbf{F}_T^S(\mathbf{F}_T^S)^T$ is the left Cauchy-Green deformation tensor. The following relations can be also derived for the components of (70),

$$J_T^S = \frac{1}{\det(\mathbf{F}_T^G)} J_T, \tag{71}$$

$$\mathbf{B}_T^S = \mathbf{B}_T(\mathbf{F}_T^G)^{-1}(\mathbf{F}_T^G)^{-T}, \tag{72}$$

$$\det(\mathbf{B}_T^S) = \det(\mathbf{B}_T) \cdot \det\left((\mathbf{F}_T^G)^{-1}(\mathbf{F}_T^G)^{-T}\right). \tag{73}$$

The remaining derivation related to Ψ^{els} is to evaluate the effect of deformation on the chemical potential (58). Taking into account that $\mathbf{F}^G$ can be a function of volume fraction, one can write,

$$\frac{\partial \Psi^{\mathrm{els}}}{\partial \phi} = \frac{\partial \Psi^{\mathrm{els}}}{\partial \mathbf{F}_T} : \frac{\partial \mathbf{F}_T}{\partial \mathbf{F}_T^G} : \frac{\partial \mathbf{F}_T^G}{\partial \phi} \tag{74}$$

[11] Experimental studies indicate that the elastic response of the soft biological tissues resembles that of rubberlike materials and polymers [39, 47, 107] and is often modeled as hyperelastic. To derive a general tumor model framework, without loss of generality, we consider a Neo-Hookean model while other hyperelastic models can be substituted, including classical models of Ogden [122, 123] and Mooney-Rivlin [115, 134] or the extended models [21, 33, 75, 130]. Another common assumption is that soft biological tissues are incompressible exhibiting viscoelastic behavior [31]. We assumed that the tumor tissue is compressible, since the porous nature of the tumor may cause significant compressibility when fluid locally migrates into or out of the tissue. It is also assumed that the tumor growth is an extremely slow phenomenon, and it is sufficient to consider a time-independent model.

where

$$\frac{\partial \mathbf{F}_T}{\partial \mathbf{F}_T^G} = \mathbf{F}_T^S \otimes \mathbf{I}\,. \tag{75}$$

Skalak *et al* [142, 143] cast the kinematics of growth into the mathematical theory of finite strain continuum mechanics through the notion of "volumetric growth". However, considering the kinematic effect of growth alone, where material is added to or lost from the body, might lead to incompatible adjacent neighborhoods of the body in Euclidean space and $\mathbf{F}^G$ cannot then be expressed as the gradient of a vector field[12]. In (64) both $\mathbf{F}^G$ and $\mathbf{F}^S$ are incompatible, but their multiplicative decomposition is compatible by construction. This multiplicative framework has been widely employed to model certain features of biological growth (e.g., [5, 6, 60, 102, 150, 166]). Nevertheless, some investigators, (e.g., [18, 76]), argued against such a decomposition based on the mass gain or loss during growth. They pointed out that if the mapping between configurations is defined only by the deformation, in the case of biological growth, the notion of a fixed reference configuration vanishes. Such a fundamental deficiency is valid for the theories of growth that consider tissue as a single-constituent solid continuum. However, the growth models based on mixture theory, where different species can possess different natural configurations, removes the challenge encountered in identifying reference configurations for the growing tissue [4].

3.2 Constitutive Relations for Deformation Feedback on Diffusion

Prior to presenting an evolution relation for the growth tensor, we first postulate the way deformation is coupled to the diffusion equation. To account for the restriction of tumor expansion produced by the surrounding tissues, one might consider the dependency of diffusion on deformation [55]. Such hypothesis testing using *in vivo* data is shown to significantly improve the predictability of computational models [74, 97, 160, 161] in addressing the experimental observations. Most of the previous models considered the dependency of the mobility tensor (i.e., the diffusion coefficient in reaction-diffusion models) to a stress quantity. However, the principle of material frame-indifference [43] shows that the mass flux can be a function of the right Cauchy-Green deformation tensor or its invariants, volume fraction, and gradient of chemical potential, such as

$$\mathbf{J}_T = \mathbf{J}_T(\mathbf{C}_T, \phi_T, \nabla \mu_T)\,. \tag{76}$$

Thus, from (56) along with considering the dependency of the tumor mobility tensor on the volume fraction [94, 96], we postulate the following form describing tumor mobility, $\mathbf{M}_T = M_T\mathbf{I}$[13],

[12]The decomposition of the deformation gradient into elastic and growth parts in (64) was first introduced in biomechanics by Rodrigez *et al* [136] to address the effects of incompatible growth.

[13]It should be noted that the relation $\nabla\mu_\alpha \cdot \mathbf{J}_\alpha \leq 0$ obtained from the rate of dissipation potential of each constituent ensures no matter how large the deformation, it cannot induce a flow of mass in the absence of a volume fraction gradient.

$$M_T = \lambda_T^{\text{mob}} \phi_T^2 (1 - \phi_T)^2 . \tag{77}$$

The double-well functional form of the dependency to the volume fraction in (77) assumes that the pure phases (i.e., just tumor ($\phi_T = 1$) or healthy cells ($\phi_T = 0$)) do not diffuse. This functional ensures the mobility is always positive and avoids possible inconsistency in the phase field model [41, 71][14]. Moreover, the inhibitory effect of the surrounding tissue on tumor growth is mimicked by an exponential decay, such as

$$\lambda_T^{\text{mob}} = \alpha_T^{\text{mob}} \exp(-\gamma_T^{\text{mob}} J_T), \tag{78}$$

where α_T^{mob} and γ_T^{mob} are constants and $J_T = \sqrt{\det(\mathbf{C}_T)}$ is a measure of volume change.

We postulate that the following source terms govern the tumor mass exchange term

$$S_T = \lambda_T^{\text{pa}} \phi_T (1 - \phi_T) \phi_\sigma . \tag{79}$$

The relation for the tumor source term addresses the biophysical processes including (i) continuous growth of the proliferating tumor cells when consuming nutrient and (ii) the tumor volume fraction levels off when reaching the volume fraction of 1. The constant rate of the cellular mitosis minus apoptosis is indicated by λ_T^{pa}, characterizing the growth in the solid phase. We thus assume that growth evolution in the mass balance, as the process of mass addition and loss, is directly related to both the tumor and nutrient-rich extracellular water volume fractions. Moreover, a relation for λ_T^{pa} is proposed to account for the mechanical effects of decreasing the rate of tumor cell proliferation with increasing the surrounding tissue stress, such as

$$\lambda_T^{\text{pa}} = \alpha_T^{\text{pa}} \exp(-\gamma_T^{\text{pa}} J_T), \tag{80}$$

where α_T^{pa} and γ_T^{pa} are constants controlling decay of the growth stretch with increasing tumor volume. The further dependency of λ_T^{pa} addresses the increase in proliferation rate in the area with high tumor cell density. The relation between proliferation rate and cell density is shown in a recent investigation using *in vitro* measurements [95].

The mobility tensor for nutrient rich water is assumed uniform throughout the domain, given as

$$\mathbf{M}_\sigma = M_\sigma \mathbf{I}, \tag{81}$$

[14]Lee *et al* [89, 90] showed that the long-time behavior of Cahn-Hilliard equation with a quadratic degenerate mobility, i.e., $M_T = 1 - \phi_T^2$ does not reduce to surface diffusion as its long-time, sharp interface limit.

where M_σ is a constant describing the nutrient mobility. The nutrient concentration decreases, as it is consumed by the tumor cells, at a rate λ_σ. Here, we neglect the natural decay and healthy cell consumption of nutrient, as we consider that the healthy cells are in homeostasis. With these assumptions, the nutrient source term is given as

$$S_\sigma = -\lambda_\sigma \phi_T \phi_\sigma, \tag{82}$$

where λ_σ is a constant.

In the current formulation, the feedback of deformation on the tumor mobility and source term is considered through a function of volume change. Even in the absence of other biological and chemical effects, there is no general agreement in the literature on whether growth processes relate best to stress or strain [4]. Here we argue that the stress is an unobservable quantity and does not directly appear in observational data to support or contradict any particular hypothesis with respect to an explicit form of the stress tensor. Thus, in the relations of tumor mobility (78), tumor mass exchange (80), and (consequently) the evolution equation of the growth stretch ratio (85), we consider a representative measure of the tumor deformation J_T, which correlates an increase or decrease in the tumor volume with the increase or decrease of the surrounding tissue induced stress to the solid tumor. While the mathematical arguments for the proposed mechanical feedback on the tumor mobility and source term are intuitive, more physics-based constitutive relation is needed based on the underlying mechanisms of such complex bio-physical phenomena from cellular and sub-cellular investigations.

3.3 Constitutive Relation for Growth Tensor

The continuum mechanics treatment of growth introduces $\mathbf{F}_T^G$ as a new unknown that is neither governed by a new balance law nor can be found based on thermodynamic arguments. Thus, a constitutive relation must be postulated for the evolution law of growth in relation to physical, biological, and chemical effects. Proposing an evolution relation for growth can follow two general approaches. Motivated from engineering materials modeling, micromechanically-based evolution equations might be considered for growing tissue. However, this approach encounters additional challenges in describing biological growth due to the requirement of *in vivo* characterization of living tissue and strong dependency of the growth law on the type of tissue under consideration. Additionally, micro-mechanical based models might lead to a large number of model parameters and challenges the predictive capability of the model due to the lack of experimental observations to calibrate and validate the model. Another approach consists of hypothesizing phenomenological laws based on experimental observations. Such models result in the development of theories that can be effectively informed by specific experiments from which model parameters can be evaluated[15]. Since a primary goal of the current formulation is to develop a tumor model that can ultimately be informed by experimental data of tumor evolution, we follow the latter approach.

[15]For instance, in many physiological systems one can consider the notion of homeostatic, indication that growth occurs in a way that minimizes the difference between the actual stress and a preferred stress, to propose a differential law for the evolution of the growth [4].

Tumor growth is taken to be anisotropic and the growth component of the deformation gradient (growth tensor) is given by

$$\mathbf{F}_T^G = \Lambda_T^G \boldsymbol{\Omega}, \tag{83}$$

where Λ_T^G is the growth stretch ratio ($\Lambda_T^G > 1$ indicates growth and $\Lambda_T^G < 1$ represents resorption) and

$$\boldsymbol{\Omega} = \begin{bmatrix} \omega_1 & & \\ & \omega_2 & \\ & & \omega_3 \end{bmatrix}, \qquad \omega_1^2 + \omega_2^2 + \omega_3^2 = 1 \tag{84}$$

is the anisotropy tensor, with ω_1, ω_2, and ω_3 being anisotropic growth multipliers [10, 11, 13, 14] and isotropic growth (see, e.g., [147, 166]) corresponds to $\boldsymbol{\Omega} = \mathbf{I}$. Such anisotropic growth allows preferential expansion of tumors in the direction of low stress and enables stress-relaxation even in the absence of viscose dissipation, a phenomenon that is observed experimentally (see, e.g., [72]).

If the mass balance equation is not included in the formulation, the evolution of the growth stretch ratio [16] can be related to the induced pressure expressed in terms of the trace of the second Piola-Kirchhoff stress [102, 150], von Mises stress [146, 147], or the Mandel stress [73]. However, a more realistic representation of the biophysical process of a growing tumor in a heterogeneous microenvironment must account for both diffusion and deformation. In a coupled diffusion and deformation setting, the growth stretch ratio Λ_T^G and creation or degradation rate of the solid tumor constituent through mass transfer must be explicitly related to one another. We have derived a relation among the growth tensor evolution and the mass exchange terms in Appendix B. According to (108), and considering a domain $\Omega \in \mathbb{R}^d (d = 1, 2, 3)$, an evolution equation for the growth stretch ratio can be written as,

$$\frac{1}{\Lambda_T^G} \frac{\partial \Lambda_T^G}{\partial t} = \frac{1}{d} \left(S_T - \nabla \cdot (\mathbf{M}_T \cdot \nabla \mu_T) \right). \tag{85}$$

As opposed to the phenomenological evolution equations of growth stretch (e.g., [125, 146, 147, 157]), the relation (85) is derived based on physically and mathematically consistent framework (inline with [7, 116]) without the requirement of introducing additional model parameters.

3.4 Summary of Governing Equations

Using the macro-force balance (12) and neglecting the body forces, the governing equation for deformation of tumor and nutrient rich water reduces to,

[16] In the absence of mass transport, the biological growth is modeled solely based on the evolution of the growth stretch ratio, see, e.g., [73, 125, 157].

$$\frac{\partial \rho_T \phi_T \mathbf{v}_T}{\partial t} + \nabla \cdot (\rho_T \phi_T \mathbf{v}_T \otimes \mathbf{v}_T) = \nabla \cdot \mathbf{T}_T, \tag{86}$$

$$\frac{\partial \rho_\sigma \phi_\sigma \mathbf{v}_\sigma}{\partial t} + \nabla \cdot (\rho_\sigma \phi_\sigma \mathbf{v}_\sigma \otimes \mathbf{v}_\sigma) = \nabla \cdot \mathbf{T}_\sigma, \tag{87}$$

where

$$\begin{aligned} \mathbf{T}_T &= \frac{1}{\Lambda_T^G}\left(\frac{G_T}{J_T^{S^{5/3}}}\left(\mathbf{B}_T^S - \frac{1}{3} tr(\mathbf{B}_T^S)\mathbf{I}\right) + K_T(J_T^S -)\mathbf{I}\right)\boldsymbol{\Omega}^{-1} \\ &- \epsilon_T \nabla \phi_T \otimes \nabla \phi_T, \end{aligned} \tag{88}$$

$$\mathbf{T}_\sigma = -p_\sigma \phi_\sigma \mathbf{I} + \frac{1}{2} A_\sigma (\nabla \mathbf{v}_\sigma + \nabla \mathbf{v}_\sigma^T). \tag{89}$$

The species mass balance relations (17) for two constituents are,

$$\frac{\partial \rho_T \phi_T}{\partial t} + \nabla \cdot (\rho_T \phi_T \mathbf{v}_T) = S_T - \nabla \cdot (\mathbf{M}_T \cdot \nabla \mu_T), \tag{90}$$

$$\frac{\partial \rho_\sigma \phi_\sigma}{\partial t} + \nabla \cdot (\rho_\sigma \phi_\sigma \mathbf{v}_\sigma) = S_\sigma - \nabla \cdot (\mathbf{M}_\sigma \cdot \nabla \mu_\sigma), \tag{91}$$

where S_T and S_σ are defined in (79) and (82), $\mathbf{M}_\sigma$ is defined in (81), the form of $\mathbf{M}_T$ is presented in (77). Neglecting the external microforce, the chemical potentials are defined as:

$$\begin{aligned} \rho_T \mu_T &= 2\kappa \phi_T (2\phi_T^2 - 3\phi_T + 1) - \chi_0 \phi_\sigma - \epsilon_T^2 \Delta \phi_T \\ &+ \frac{J_T}{\Lambda_T^G} \frac{\partial \Lambda_T^G}{\partial \phi_T} (\mathbf{T}_T + \epsilon_T \nabla \phi_T \otimes \nabla \phi_T) : \mathbf{I}, \end{aligned} \tag{92}$$

$$\rho_\sigma \mu_\sigma = 2\frac{1}{\delta_\sigma}\phi_\sigma - \chi_0 \phi_T. \tag{93}$$

Differential equations (86), (87), (90), and (91), characterize the coupled diffusion and hyperelastic deformation of tumor growth. Additionally, Ambrosi and Mollica [6] argue that in the case of biological tissues, the characteristic velocities are so small that the process can be conveniently modeled as quasi-static. Assuming the velocities of tumor and nutrient rich extra cellular water are negligible ($\mathbf{v}_T \approx 0$ and $\mathbf{v}_\sigma \approx 0$) and considering isotropic growth ($\mathbf{F}_T^G = \Lambda_T^G \mathbf{I}$), the following (simplified) system of partial differential equation for mass balance and deformation equations is obtained,

$$\left.\begin{aligned}
\frac{\partial \phi_T}{\partial t} &= S_T - \nabla \cdot (M_T \nabla \mu_T), \\
\mu_T &= 2\kappa \phi_T (2\phi_T^2 - 3\phi_T + 1) - \chi_0 \phi_\sigma - \epsilon_T^2 \Delta \phi_T \\
&\quad + \frac{J_T}{\Lambda_T^G} \frac{\partial \Lambda_T^G}{\partial \phi_T} \mathbf{T}_T : \mathbf{I}, \\
\frac{\partial \phi_\sigma}{\partial t} &= S_\sigma - \nabla \cdot (M_\sigma \nabla \mu_\sigma), \\
\mu_\sigma &= 2\frac{1}{\delta_\sigma} \phi_\sigma - \chi_0 \phi_T, \\
\nabla \cdot \mathbf{T}_T &= 0 .
\end{aligned}\right\} \tag{94}$$

In the above relations, it is also assumed that the mass density of the tumor and nutrient are constant, thus ρ_T and ρ_σ do not appear in mass balances. For the numerical experiments, the governing equations of the four-species mixture models in (94) are numerically approximated using finite elements formulation by developing a new solution algorithm (see Appendix C).

4 Numerical Results

In this section, the results of numerical experiments are discussed to investigate the main features of the proposed model. The numerical analyses are conducted on a tumor growing on the domain $\Omega = [-1, 1]^2$ with an ellipsoidal shaped initial tumor subdomain in the center of Ω,

$$\left\{(x, y) : \frac{x^2}{0.8} + \frac{y^2}{1.1} \leq 0.2^2\right\}. \tag{95}$$

In all numerical experiments, a regular triangular mesh with 6400 elements and $\Delta t = 0.05$ selected to ensure spatial and temporal accuracy. The parameter values used in the numerical experiments are shown in Table 1. We present the simulation results of four different cases. In one set of numerical experiments, the initial nutrient volume fraction is taken to be uniform, while in the other set a nutrient gradient is initially prescribed. For each initial nutrient scenario, the effect of mechanical stress feedback on tumor growth is investigated by considering two cases: *unconfined growth* representing freely growing tumor without the effects of the surrounding tissue characterized by $\gamma_T^{pa} = \gamma_T^m = 0$, and *confined growth* indicating the inhibitory effect of the externally applied stress on the growing tumor by assigning $\gamma_T^{pa} = \gamma_T^m = 1$. The motivation for choosing these cases is *in vitro* data obtained from multicellular tumor spheroid experiments [3, 30, 72, 127, 163], in which the tumor cells are cultured in a matrix (polymeric gel). Such *in vitro* models mimic the confinement induced by the tumor environment (surrounding tissues) and enable systematic investigation of the externally applied stresses on tumor growth. These studies show that the mechanical properties of the surrounding matrix have a significant influence on the proliferation and

migration of tumor cells [3, 30, 127, 163]. We aim to investigate the capability of the developed mixture model by simulating the underlying phenomena observed in these experiments through the mechanical stress feedback on the development of the tumor.

4.1 Uniform Initial Nutrient Volume Fraction

The first set of the numerical experiments are conducted by assigning a spatially uniform nutrient distribution (ϕ_σ=0.5) as the initial condition and imposing no flux boundary conditions of Neumann type on ϕ_T, μ_T, and μ_σ and Dirichlet conditions on ϕ_σ and displacement $\mathbf{u}_T$:

$$\left.\begin{array}{lll} \nabla\phi_T\cdot\mathbf{n}=0 & , & \nabla\mu_T\cdot\mathbf{n}=0 \\ \phi_\sigma=0.5 & , & \mathbf{u}_T=0 \end{array}\right\} \quad \text{on } \Gamma$$

where Γ is the Lipschitz boundary of Ω and **n** is a unit exterior normal vector on Γ. The snapshots of the tumor and nutrient volume fractions for the confined (panels A-F) and unconfined (panels G-L) tumor growth are shown in Figure 1. In both cases, the tumor volume fraction uniformly increases over time while the nutrient is consumed in the center of the tumor. However, including the effect of mechanical feedback of the surrounding tissue on tumor development in the confined case, results in reducing the growth rate leading to 70.82% smaller tumor area[17] at the final simulation time t=12.5. These results are in agreement with the *in vitro* models of tumor cells growth within a polymer gel, in which increasing the gel stiffness inhibits tumor growth by reducing tumor cell proliferation and inducing apoptosis [30, 72, 87].

It is important to note that the proposed theory couples two mechanisms of tumor growth governed by the source term S_T in the diffusion equation of tumor (79), and the growth stretch ratio Λ_T^G that evolves according to (85). In a finite element simulation, the former mechanism corresponds to occupying more elements with the tumor volume fractions, while the latter growth mechanism results in the tumor elements stretch. Both mechanisms affect the rate of increase in tumor area and are controlled by the term λ_T^{pa} according to (80). Thus, the postulated exponential decay with the model parameters γ_T^{pa} and α_T^{pa} represents the property of the tumors surrounding environment that regulates the externally applied stress. For instance, higher values of the model parameter γ_T^{pa} lowers the rate of tumor area expansion with time by simulating stronger confinement induced by the surrounding tumor environment.

Figure 2 presents the spatial distributions of the growth stretch ratio Λ_T^G (panels A and D), the normal component of the Cauchy stress along x-axis T_{xx} (panels B and E), and the magnitude of the Cauchy stress tensor |**T**| in the tumor and surrounding host tissue (panels C and F) for unconfined (top row) and confined scenarios (bottom row), respectively. The spatial profiles of the tumor growth stretch ratio[18] in these figures show a higher growth rate

[17]The numerical values provided in this section correspond to the numerical experiments conducted using the model parameters in Table 1.

in the periphery of the tumor (a ring close to the interface of tumor and surrounding tissues) with 10.97% higher Λ_T^G in periphery compared to tumor interior at t=12.5. This response can be explained by the spatial distribution of nutrients and its evolution throughout tumor development. As observed in experiments [30, 147], during the avascular stage of tumor growth, the supply of nutrients from the environment is transported to the tumor interior *via* diffusion. This process leads to a gradient of nutrient concentration, and an associated gradient in growth rate, from the periphery to the interior of the tumor. The simulation results of nutrient volume fraction (Figure 1) and the growth stretch ratio (Figure 2) indicate that the proposed model is able to capture this physical process. Aligned with simulations from multiscale agent-based models [103, 121, 135], the formation of a ring in the Λ_T^G profile that varies radially in space suggests that the periphery contains the proliferative tumor cells while the quiescent and necrotic cells are in the tumor interior, depending on the nutrient availability. Figure 3 shows the time evolution of tumor area normalized by the domain area. For these plot, a larger domain size $\Omega = [-2.5, 2.5]^2$ is employed to allow larger tumor size. The results of unconfined growth indicate that after the initial period of monotonic growth the rate of increase in tumor area reduces with time. Such responses suggest that the avascular tumor may not always grow indefinitely even in the absence of external confinement [6, 7, 165, 166]. Such a decrease in the growth rate can occur when the rate of tumor growth overcomes the nutrient transport characterized by M_σ, known as *diffusion-limitation* in avascular tumor growth [109, 111, 117]. This phenomenon leads to an avascular tumor reaching a steady-state size, which corresponds to a balance between proliferation and apoptosis and agrees with both *in vivo* and *in vitro* experiments [3, 72, 88, 108, 110, 148]. In principle, the non-uniform distribution of nutrients leads to heterogeneous growth, and hence, the generation of residual stress retained inside the tumor that inhibits tumor cell proliferation [4, 17, 46, 147]. However, it is shown that the stress field generated in unconfined growth does not considerably impact the size of the tumor, compared to the surrounding tissue confinement [7, 78].

The Cauchy stress profiles in Figure 2 (panels C and F) indicate that, in both confined and unconfined scenarios, the stress magnitude is higher in the tumor periphery compared to the interior of the tumor. The ratios of the average $|\mathbf{T}|$ in the periphery to interior regions are approximately 9.1 for the unconfined and 15.5 for the confined cases at the final time t=12.5. The simulation results of T_{xx} show that in the radial direction (along y-axis) the stress within tumor interior area is compressive (negative sign) and they diminish radially in space at the interface of the tumor with the surrounding tissue. However, the stress in the circumferential direction (T_{xx} along the x-axis) is compressive and spatially uniform within the tumor interior, and it turns to tensile (positive sign) at the periphery. Such stress developments are also important in the vascular stage of tumor growth in which the compressive stress in the tumor interior can collapse blood vessels. Additionally, competition among compressive and tensile stresses at the interface of the tumor and normal tissue may result in deformation of peritumoral vessels [124, 147].

[18]We note that $\Lambda_T^G = 1$ in the surrounding tissue.

Comparing the growth stretch ratio and the Cauchy stress developments in confined and unconfined growth scenarios (Figure 2, panels A and D) shows the remarkable regulatory effect of the externally applied stress. Such stress induced by the surrounding tissue on tumor cell proliferation suppresses the growth rate and reduces the stress development in the solid tumor. The formation of a highly proliferative ring in the Λ_T^G profile and the effect of surrounding tissue confining stress applied on tumor shown in Figure 2 are in agreement with experimental observations [3, 30, 113, 114] and analytical studies under fully symmetric spherical growth assumption [7, 46, 78, 138, 140, 165]. The physical phenomena captured by the proposed model, naturally arise from the phase development of the tumor and mathematical consistency among the growth tensor and mass exchange, without any ad hoc introduction of these processes. Additionally, the current phase-field mixture model accounts for the surface tension-like force (due to cell-cell adhesion) at the interface of the tumor and healthy constituents. Such microscopic force is controlled by the interface thickness parameter ϵ_T, and promotes the higher compressive stress in the tumor periphery (see [43] for numerical results of the evolution of adhesion force). In this regard, the proposed theory accounts for the nonlocal cell adhesion effect on the solid tumor stress and enables capturing the responses of high adhesion (e.g., epithelial tumors [156]) and low adhesion and higher motility cells (e.g., glioblastoma and stromal tumors [84, 104, 133]).

4.2 Spatially Varying Initial Nutrient Volume Fraction

In the second set of the numerical experiments, we investigate the role of the chemotactic term on the evolution of the tumor growth. In this case, we considered the following boundary condition at the top and bottom boundaries of the domain, Γ_{tb},

$$\left.\begin{array}{ll} \nabla\phi_T\cdot\mathbf{n}=0 & , \quad \nabla\mu_T\cdot\mathbf{n}=0 \\ \nabla\phi_\sigma\cdot\mathbf{n}=0 & , \quad \mathbf{u}_T=0 \end{array}\right\} \quad \text{on } \Gamma_{\text{tb}}.$$

However, on the left and right boundaries Γ_{lr}, Dirichlet boundary conditions are imposed on ϕ_σ to create a nutrient gradient along x direction,

$$\left.\begin{array}{ll} \nabla\phi_T\cdot\mathbf{n}=0 & , \quad \nabla\mu_T\cdot\mathbf{n}=0 \\ \phi_\sigma=0.1 \text{ and } 0.9 & , \quad \mathbf{u}_T=0 \end{array}\right\} \quad \text{on } \Gamma_{\text{lr}},$$

with nutrient volume fraction of ϕ_σ=0.1 at the left boundary, and ϕ_σ=0.9 at the right boundary. With these boundary conditions, the scenario mimics the effects of a nutrient source (for example a blood vessel) on the right side of the tumor.

Figure 4 shows snapshots of tumor and nutrient volume fractions, at t = 0.5, 5.0, 12.5. According to (61), the nutrient acts as a chemoattractant in the proposed model; that is, the diffusion of the tumor volume fraction is strengthened by nutrient gradients. As a result of this effect, in both the confined and unconfined cases, the tumor grows towards the direction of higher nutrient concertation (right boundary) [49, 54, 96]. Over time, the chemotactic effect results in a non-symmetric shape of the tumor in which the right interface between the tumor and healthy cells has approximately 60% higher thickness. Higher thickness of the tumor interface captures the increase of the tumor proliferation at the higher nutrient

environment. These figures indicate that the proposed mixture theory can characterize the development of heterogeneous morphology and invasive patterns as observed in both *in vivo* and *in vitro* experiments [52, 129, 162, 168]. Similar to the uniform initial nutrient scenario, the inhibitory effect of the surrounding tissue stress on tumor development in the confined case (Figure 4, bottom two rows) reduces the growth rate leading to 71.04% reduction in tumor area at the final time t=12.5. Additional numerical experiments show that the intensity of tumor cells migration towards nutrient sources is proportional to the value of the chemotactic parameter χ_0.

The spatial distributions of the Λ_T^G, T_{xx}, and |**T**|, for the spatially varying nutrient scenario, is shown in Figure 5. As expected, the proliferative tumor cells tend to concentrate on the higher nutrient area, leading to approximately 45% thicker proliferation ring with 2.75% higher value of growth stretch ratio on the right side compared to the left side of the simulated tumor periphery at t=12.5. In these figures, the compressive Cauchy stress in the tumor interior remains the same compared to the uniform nutrient scenario. However, 41.3% higher tensile circumferential stress in the tumor periphery region is observed in the right side of the tumor. Additionally, in the confined case (Figure 5, panels D, E, and F), the tumor cell proliferation is suppressed in the direction of higher mechanical stress, in agreement with experimental observations [30].

5 Discussion

We have developed a general mixture theory for mass transfer of multiple constituents to address the key mechano-chemo-biological mechanisms involved in avascular tumor growth at the tissue scale, while accounting for certain phenomena at the cellular scale. The local species mass balance relations result in a system of fourth-order parabolic partial differential equations of the Cahn-Hilliard type to be solved together with the deformation differential equations incurred by the macro-force balances. These equations, along with appropriate boundary and initial conditions, characterize a general, coupled phase-field and hyper-elastic deformation, continuum mixture model of a complex media consisting of multiple solid and fluid species. The constituents can be compressible, the fluid species are Newtonian, the solid constituents are isotropic hyperelastic, and the effects of diffusion of chemical or biological constituents due to chemo- or bio-taxis, as well as surface effects due to cell adhesions, are considered. We then specialized the general framework to describe the response of a mixture consisting of four constituent volume fractions: tumor cells, nutrient-rich extracellular water, nutrient-poor extracellular water, and healthy cells. We were particularly interested in modeling biological and chemical factors, as well as the mechanical cues to tumor cells and their link with tissue level tumor progression. In addition to mass transfer, the growth effects and its interaction with the deformation are included in this model through the decomposition of the tumor deformation gradient into elastic and growth components. To fully characterize the biological growth in relation to mechanical, biological, and chemical effects, constitutive relations were postulated for the tumor growth while accounting for the deformation feedback on the mass transfer processes. In particular, we proposed phenomenological constitutive models accounting for the mechanical effect of decreasing the rate of tumor cell proliferation with increasing tumor volume. In this regard,

the mobility tensor and mass exchange source term in the diffusion equations of the tumor species is considered as a decay function of the tumor of volume change indicating the increase/decrease of induced pressure from surrounding tissues. Both the diffusion source term and the growth deformation gradient tensors characterize the cancer cell proliferation and apoptosis. As a result of this physical feature, an evolution equation is derived for the growth part of the deformation gradient as a function of mass exchange terms. The differential equation relating the growth stretch ratio and the mass growth rate ensure the mathematical consistency of the tumor growth model.

Numerical experiments are conducted by means of the finite element solution of the model. The computational results on the spatio-temporal evolution of simulated tumors reveal a number of important capabilities of the proposed theory in capturing key features of avascular tumor growth. In particular, it is demonstrated that the directional movement of tumor cells towards the nutrient supply, due to the chemotactic effect, results in asymmetric morphology of the tumors from the initially symmetric shape. It is also shown that stress in the tumor interior is compressive while the stress is tensile at the interface of the tumor and surrounding tissue. Additionally, the evolution of the growth deformation gradient indicates a higher growth rate in the periphery region of the tumor compared to the tumor interior. The evolutions of the stress and growth stretch ratio denote the inhibitory effect of the externally applied stress induced by the surrounding tissue on tumor cell proliferation. Accordingly, the proposed model is capable of describing the critical mechano-chemo-biological features of avascular tumor growth in the various microenvironment of living tissue, in agreement with the experimental studies in the literature [3, 30, 72, 87, 88, 148].

The proposed theoretical framework of tumor growth is built on the previous diffusion-based models of tumor growth in the microenvironment, e.g., [6, 35, 57, 76, 102, 120, 160], as well as purely mechanical models simulating the effect of macroscopic mechanical stress on the tumor cell proliferation, e.g., [10, 46, 92, 125, 143, 147, 165, 166], in the literature. The current contribution advances the previous efforts by developing a fully coupled deformation and mass transfer model, based on phase-field mixture theory, to address the fundamental governing equations of biological growth. In this regard, the proposed model provides a unified mathematical framework for simulating major biophysical phenomena encountered in tumor progression, in a thermodynamically consistent fashion. Several important physical processes captured by the proposed model naturally arise from the mathematical derivations, without any ad hoc introduction of these processes. For example, following a phase-field approach and recognizing the existence of microscopic force balances in the current theory, results in the incorporation of the stress developments due to tumor cell adhesion at the interface of tumor and surrounding phases. Additionally, the formation of the proliferative ring in the periphery region of a tumor inherently arises from the consistency of the evolution equation of the growth deformation gradient with the nutrient driven biological growth characterized by the mass transfer.

Although the proposed model addresses critical mechanisms in tumor development including the coupling of stress and growth, future investigations are required to overcome the limitations of the constitutive models. While the mathematical arguments for the mechanical feedback on tumor development are intuitive, the proposed constitutive relation

is a starting point for describing complex biological events involved in biological growth. Perhaps, identification of appropriate evolution equations for the growing mass is one of the most challenging problems in biomechanics and mechanobiology. The postulated constitutive relations for the inhibitory effect of mechanical stress on tumor cell proliferation, as a function of a deformation measure, needs to be examined and enhanced with clear biomechanical interpretations as underlying mechanisms of this phenomena that are merging from cellular and sub-cellular investigations. Furthermore, considering that the tumor growth is both organ and patient-specific, future insights from both theory and experiment are needed to validate and refine the constitutive models proposed in this contribution. Further areas to be explored are assessing the predictive capabilities of the proposed model concerning the *in vivo* measurements of cancer development as well as investigating the influence of organ confinement on tumor growth [101]. Additionally, extending the computational implementation to isolate mechanical interactions among cancer cells and the environment enables studying a range of phenomena observed in *in vitro* tumor spheroids under stress [72, 108, 110]. Important avascular tumor responses to be investigated using this model include the non-sphericity of tumor morphology growing in stiffer mechanical environment [109], as well as stress-driven cell migration, proliferation, and death [30, 46].

6 Conclusions

We have developed a general thermodynamically consistent theory, based on multispecies phase-field methods to address the multiphysics and multiscale mechanisms involved in tumor growth in a heterogeneous microenvironment. The proposed theory provides a unified mathematical framework for developing high-fidelity tumor growth models by considering, for example, the interactions among various tumor constituents, angiogenesis phenomena, and the effect of different therapeutic strategies.

Acknowledgments

We thank the National Cancer Institute for funding *via* U01CA174706 and R01CA186193. We thank CPRIT for funding *via* RR160005. We benefited from discussion with Dr. Regina Almeida, of the National Laboratory for Scientific Computing, Brazil and Dr. Aaron Baker, of the University of Texas at Austin for many informative discussions on the modeling of the effect of mechanical stress on the biological growth.

Appendices

A Deriving Force Balances From The Principles of Virtual Power

An alternative approach to determine the associated balance of macroscopic and microscopic forces is to use the principle of virtual power; see, e.g., [58, 63]. The main feature of this classical principle is a physical structure involving thermodynamic conjugate forces through the manner in which they expend power. This allows one to use the virtual-power principle to determine local and nonlocal force balances when the forms of the balances are not known *a priori* and provide a foundation to build more general theories; see, e.g., [44, 64, 65, 158].

The form of the power expenditure is determined by the terms contributing to the energy sources and postulated in the first and second laws of thermodynamics. In this regard, the internal virtual power is expressed in terms of the energy contribution in $\mathscr{R}_t$ such as

$$\mathscr{P}_{\text{int}} = \sum_{\alpha} \int_{\mathscr{R}_t} \left(\mathbf{T}_\alpha : \mathbf{D}_\alpha - \pi_\alpha \frac{d^\alpha \phi_\alpha}{dt} + \boldsymbol{\xi}_\alpha \cdot \nabla \left(\frac{d^\alpha \phi_\alpha}{dt} \right) \right) dV \,. \tag{96}$$

The internal power is balanced by the power expended by traction $\mathbf{t}_\alpha$ on the surface $\partial \mathscr{R}_t$ and body force $\mathbf{b}_\alpha$ acting within the body to account for the inertia,

$$\mathscr{P}_{\text{ext}} = \sum_{\alpha} \left\{ \int_{\partial \mathscr{R}_t} \mathbf{t}_\alpha \cdot \mathbf{v}_\alpha dA + \int_{\mathscr{R}_t} (\rho_\alpha \phi_\alpha \mathbf{b}_\alpha \cdot \mathbf{v}_\alpha - \tau_\alpha \frac{d^\alpha \phi_\alpha}{dt}) dV + \int_{\partial \mathscr{R}_t} m_\alpha \frac{d^\alpha \phi_\alpha}{dt} dA \right\}. \tag{97}$$

To account for the microscopic boundary conditions that arise from the volume fraction gradients, it is further assumed here that the external power is affected by the micro traction m_α that is a force conjugate to the time change of volume fractions on constituent interfaces [68, 120]. If we define virtual velocity to be $(\tilde{\mathbf{v}}_\alpha, d^\alpha \tilde{\phi}_\alpha / dt)$ and write (96) and (97) for the corresponding internal and external expenditures of virtual power, then the principle of virtual power is the requirement that the virtual power balance $\mathscr{P}_{\text{int}} = \mathscr{P}_{\text{ext}}$ be satisfied for any subregion $\mathscr{R}_t$ of the deformed body and any virtual velocity $\mathscr{V}$. Using the divergence theorem,

$$\begin{aligned} \int_{\mathscr{R}_t} \mathbf{T}_\alpha : \tilde{\mathbf{L}}_\alpha dV &= \int_{\partial \mathscr{R}_t} (\mathbf{T}_\alpha \mathbf{n}) \tilde{\mathbf{v}}_\alpha dA - \int_{\mathscr{R}_t} (\nabla \cdot \mathbf{T}_\alpha) \tilde{\mathbf{v}}_\alpha dV, \\ \int_{\mathscr{R}_t} \boldsymbol{\xi}_\alpha \cdot \nabla \left(\frac{d^\alpha \tilde{\phi}_\alpha}{dt} \right) dV &= \int_{\partial \mathscr{R}_t} (\boldsymbol{\xi}_\alpha \cdot \mathbf{n}) \frac{d^\alpha \tilde{\phi}_\alpha}{dt} dA - \int_{\mathscr{R}_t} (\nabla \cdot \boldsymbol{\xi}_\alpha) \frac{d^\alpha \tilde{\phi}_\alpha}{dt} dV, \end{aligned}$$

and substituting into (96), along with equating the external power to the internal power $(\mathscr{P}_{\text{int}} = \mathscr{P}_{\text{ext}})$, results in,

$$\begin{aligned} \sum_{\alpha} \Bigg\{ \int_{\partial \mathscr{R}_t} (\mathbf{T}_\alpha \mathbf{n} - \mathbf{t}_\alpha) \tilde{\mathbf{v}}_\alpha dA + \int_{\mathscr{R}_t} (-\nabla \cdot \mathbf{T}_\alpha - \rho_\alpha \phi_\alpha \mathbf{b}_\alpha) \tilde{\mathbf{v}}_\alpha dV + \\ \int_{\mathscr{R}_t} (-\pi_\alpha - \tau_\alpha - \nabla \cdot \boldsymbol{\xi}_\alpha) \frac{d^\alpha \tilde{\phi}_\alpha}{dt} dV + \int_{\partial \mathscr{R}_t} (\boldsymbol{\xi}_\alpha \cdot \mathbf{n} - m_\alpha) \frac{d^\alpha \tilde{\phi}_\alpha}{dt} \Bigg\} dA = 0 \,. \end{aligned} \tag{98}$$

Since $\mathscr{R}_t$ and virtual velocities are arbitrary, the microscopic and macroscopic force balances and traction conditions follow form (98),

$$\text{macroforce balance}: \quad \nabla \cdot \mathbf{T}_\alpha + \rho_\alpha \phi_\alpha \mathbf{b}_\alpha = 0, \tag{99}$$

$$\text{microforce balance}: \quad \pi_\alpha + \tau_\alpha + \nabla \cdot \boldsymbol{\xi}_\alpha = 0, \tag{100}$$

$$\text{macrotraction condition}: \quad \mathbf{t}_\alpha = \mathbf{T}_\alpha \mathbf{n}, \tag{101}$$

$$\text{microtraction condition}: \quad m_\alpha = \boldsymbol{\xi}_\alpha \cdot \mathbf{n}\,. \tag{102}$$

As indicated previously, the microforces π_a, τ_a, and $\boldsymbol{\xi}_a$ are generalized forces that arise due to nonlocality encountered in the evolution of phase boundaries [68, 83][19]. In the context of biological events responsible for the growth of a tumor, these terms represent the power expended by the interaction and adhesion between cell concentrations due to rates of change of each volume fraction on the surface of the full mixture [35, 164].

The relations (99) - (102) demonstrate the consequence of the principle of virtual power. This shows that after postulating the proper form of energy balance law, the virtual power balance encapsulates the local force balance (12) as well as additional balance laws representing the events in smaller scales (15). In particular, without assuming *a priori* that the force and momentum balance laws are satisfied, they are derivable from another hypothesis; i.e., the principle of virtual power. Requiring the internal power $\mathscr{P}_{\text{int}}$ to be frame-indifferent, eliminates the need to impose a balance of angular moments.

B Growth Tensor and Mass Exchange Rate

The fundamental governing equation of biological growth, as the process of mass addition and loss, is the mass balance written in terms of the order parameter, i.e., volume fraction in the current formulation. This diffusion equation is necessary to address the physical phenomena involved in macroscopic growth. In the case of coupled diffusion-deformation formulation, an evolution equation of the growth tensor must be consistent with the growth characterization through the mass transfer equation (i.e., mass supply and flux). Here we derive a relation between growth tensor $\mathbf{F}_T^G$ and mass exchange rate under the isotropic growth assumption[20],

$$\mathbf{F}_T^G = \Lambda_T^G \mathbf{I}\,. \tag{103}$$

Considering a two phase mixture with volume v in which a solid phase (tumor) undergoes pure growth process $\mathbf{F}_T^S = 0$. In this case, the volume occupied by tumor constituent increases from initial value $v_T^0 = v_T(t_0)$ to a volume $v_T(t)$ in time t. The volume change due to this growth process is,

[19]Using the principle of frame-indifference and the requirement that the internal power be invariant to changes in frame, it can be shown (see [43]) that the $\boldsymbol{\xi}_a$ are frame-indifferent and the Cauchy stress $\mathbf{T}_a$ is both frame-indifferent and symmetric. The symmetry of the Cauchy stress is also concluded from the balance of the angular momenta in (13).

[20]The assumption of isotropic/homogeneous growth is only valid for small avascular tumors. For vascular tumors, that display heterogeneous anisotropic growth, the growth tensor must be anisotropic.

$$J_T^G = \frac{dv_T}{dv_T^0}. \tag{104}$$

Following (103), the change in the tumor volume can be also represent as,

$$J_T^G = \det(\mathbf{F}_T^G) = (\Lambda_T^G)^3. \tag{105}$$

Equating above relations along with the definition of tumor volume fraction (5), results in following relation consistent with the formulation developed by Garikipati *et al* [56, 57, 116],

$$\Lambda_T^G = \left(\frac{\rho_T \phi_T}{\rho_T^0 \phi_T^0}\right)^{1/3}, \tag{106}$$

where $\phi_T^0 = \phi_T(t_0)$ and $\rho_T^0 = \rho_T(t_0)$.

Additionally, the tumor mass balance under quasi-static assumption is

$$\frac{\partial \rho_T \phi_T}{\partial t} = S_T - \nabla \cdot (\mathbf{M}_T \cdot \nabla \mu_T). \tag{107}$$

Substituting $\rho_T \phi_T$ from (106) into above relation, one can find an evolution equation for growth stretch ratio as,

$$\rho_T^0 \phi_T^0 \frac{\partial (\Lambda_T^G)^3}{\partial t} = \rho_T \phi_T (S_T - \nabla \cdot (\mathbf{M}_T \cdot \nabla \mu_T)). \tag{108}$$

The above equation provides a consistent framework to determine the growth tensor evolution equation from functional forms of S_T and M_T postulated based upon biophysical phenomena. A similar relation is presented by Ambrosi and Mollica using a consistent mathematical derivations based on the natural configuration argument and Lagrangian form of the mass balance(for more details see [6, 7]).

C Finite Element Formulation

C.1 Semi-implicit Time-discretization Scheme

Because of both the bilaplacian operator and the nonlinearity of the Cahn-Hilliard-type tumor diffusion equations the development of stable time-discretization scheme is a non trivial challenge. For the proposed model, we make use of a first-order accurate unconditional energy-stable scheme for gradient-flow systems based on the splitting of the non-mechanical part of the Helmholtz free energy,

$$\Psi = \frac{\epsilon_T^2}{2} \mid \nabla \phi_T \mid^2 + \kappa \phi_T^2 (1 - \phi_T)^2 + \frac{1}{2\delta_\sigma} \phi_\sigma^2 - \chi_0 \phi_T \phi_\sigma \tag{109}$$

into a convex (contractive) and concave (expansive) part,

$$\Psi = \Psi_c + \Psi_e \,. \tag{110}$$

The idea of the energy splitting scheme is to treat the contracting, more stable, part implicitly and the expanding part explicitly. Following [71, 96], one can write the following split of the free energy,

$$\Psi_c = \frac{3}{2} \kappa \phi_T^2 + \frac{\epsilon_T^2}{2} \mid \nabla \phi_T \mid^2 - \chi_0 \phi_T \phi_\sigma, \tag{111}$$

$$-\Psi_e = \kappa (\phi_T^4 - 2\phi_T^3 - \frac{1}{2} \phi_T^2) \,. \tag{112}$$

Thus, dividing the time domain into n time step of size $\Delta t = t_{n+1} - t_n$, the time stepping scheme in the tumor chemical potential can be represented as,

$$\begin{aligned} \mu_{T_{n+1}} &= \frac{\partial \Psi_c(\phi_{T_{n+1}})}{\partial \phi_T} - \frac{\partial \Psi_e(\phi_{T_n})}{\partial \phi_T}, \\ &= 3\kappa \phi_{T_{n+1}} - \chi_0 \phi_{\sigma_{n+1}} - \epsilon_T^2 \Delta \phi_{T_{n+1}} - \kappa (4\phi_{T_n}^3 - 6\phi_{T_n}^2 - \phi_{T_n}) \end{aligned} \tag{113}$$

C.2 Finite Element Solution of the Nonlinear System

The finite element solution for the coupled nonlinear system of equations (94) is obtained by uncoupling the equation according to Algorithm 1. Newton's method is employed to solve each set of equations. To define the finite element space relevant to (94), we consider homogeneous Neumann boundary conditions for all variables. Let $\mathscr{V}$ being a Hilbert space consisting of functions of time with values in $H^1(\Omega)$. We define the finite-dimensional spaces $\mathscr{V}^h$ by,

$$\mathscr{V}^h = \{ v^h \in H^1(\Omega) : v^h \mid_\tau = \hat{v} \circ F_\tau, \hat{v} \in Q_1, \tau \in \mathscr{T}^h \}, \tag{114}$$

where $\mathscr{T}^h$ is a quasi-uniform family of triangulations of Ω, F_τ is an affine map from the master element $\hat{\tau}$ to τ, and Q_1 is the tensor product of polynomials of degree 1. Let $(\cdot, \cdot)$ denote the $L^2(\Omega)$-inner product with $(u, v) = \int_\Omega uv dx$ (see [119] for details).

The weak formulation for the nutrient diffusion considering v_σ as test function is given by

$$\begin{aligned}&\text{Find } \phi_{\sigma_{n+1}} \in \mathscr{V}^h, \forall v_\sigma \in \mathscr{V}^h:\\&(\phi_{\sigma_{n+1}} - \phi_{\sigma_n}, v_\sigma) - \Delta t(S_\sigma(\phi_{T_n}, \phi_{\sigma_{n+1}}), v_\sigma)\\&- \Delta t(M_\sigma \nabla \mu_\sigma(\phi_{T_n}, \phi_{\sigma_{n+1}}), \nabla v_\sigma) = 0\,.\end{aligned} \tag{115}$$

We consider a mixed variational formulation of Cahn-Hilliard equation of tumor diffusion involving both ϕ_T and μ_T as separate unknowns. Applying the semi-implicit time-stepping scheme, the weak formulation for the tumor diffusion, considering v_T and q_T as test functions, is defined as

$$\begin{aligned}&\text{Find } (\phi_{T_{n+1}}, \mu_{n+1}) \in \mathscr{V}^h \times \mathscr{V}^h, \forall v_T, w_T \in \mathscr{V}^h:\\&(\phi_{T_{n+1}} - \phi_{T_n}, v_T) - \Delta t\,(S_T(\phi_{T_{n+1}}, \phi_{\sigma_{n+1}}, J_{T_n}), v_T)\\&- \Delta t\,(M_T(\phi_{T_{n+1}}, J_{T_n}) \nabla \mu_{T_{n+1}}, \nabla v_T) = 0,\end{aligned} \tag{116}$$

$$\begin{aligned}&(\mu_{T_{n+1}}, w_T) + \Delta t\,(3\kappa\phi_{T_{n+1}} - \chi_0\phi_{\sigma_{n+1}} - \epsilon_T^2\Delta\phi_{T_{n+1}}, w_T)\\&- \Delta t\,(\kappa(4\phi_{T_n}^3 - 6\phi_{T_n}^2 - \phi_{T_n}), w_T)\\&+ \frac{J_{T_n}^S}{d}(\Lambda_T^G)_n^3 \Delta t(\mathbf{T}_{T_n}, w_T) = 0\,.\end{aligned} \tag{117}$$

Having $\phi_{T_{n+1}}$, the growth stretch ratio can be updated using the discretized evolution equation (85), as

$$\begin{aligned}&\text{Find } (\Lambda_T^G)_{n+1} \in \mathscr{V}^h:\\&(\Lambda_T^G)_{n+1} = (\Lambda_T^G)_n + \frac{1}{d}(\Lambda_T^G)_n[\phi_{T_{n+1}} - \phi_{T_n}]\,.\end{aligned} \tag{118}$$

Finally, the weak formulation for the tumor deformation considering v_u as test function is given by

$$\begin{aligned}&\text{Find } \mathbf{u}_{n+1} \in (\mathscr{V}^h)^d, \forall \boldsymbol{v}_u \in (\mathscr{V}^h)^d:\\&(\mathbf{T}_T(\mathbf{u}_{T_{n+1}}, \phi_{T_{n+1}}), \nabla \boldsymbol{v}_u) = 0\,.\end{aligned} \tag{119}$$

Algorithm 1 summarizes the solution procedure using Newton iteration to solve the weak formulations.

Algorithm 1: Algorithm to solve the decoupled system of equations governing the four species tumor model.

Input: $\phi_T, \mu_T, \phi_{\sigma_0}, (\Lambda_T^G)_0, \mathbf{u}_0$

Output: $\phi_{T_n}, \mu_{T_n}, \phi_{\sigma_n}, (\Lambda_T^G)_n, \mathbf{u}_n$

begin
- $n \leftarrow 0$
- **repeat**
  - Solve $\phi_{\sigma_{n+1}}$ from (115) given $\phi_{T_n}, \phi_{\sigma_n}$
  - Solve $\phi_{T_{n+1}}$ and $\mu_{T_{n+1}}$ from (116) given $\phi_{T_n}, \phi_{\sigma_{n+1}}, \mathbf{u}_n, (\Lambda_T^G)_n$
  - Update $(\Lambda_T^G)_{n+1}$ form (118) given $\phi_{T_n}, \phi_{T_{n+1}}, (\Lambda_T^G)_n$
  - Solve $\mathbf{u}^{n+1}$ from (119) given $(\Lambda_T^G)_{n+1}, \mathbf{u}_n$
  - $n \leftarrow n+1$
- **until** $n\Delta t > T_{\max}$

References

[1]. Abdollahi B, Dunlap N, and Frieboes HB. Bridging the gap between modeling of tumor growth and clinical imaging In Abdomen and Thoracic Imaging, pages 463–487. Springer, 2014.

[2]. Adam JA. General aspects of modeling tumor growth and immune response In A survey of models for tumor-immune system dynamics, pages 15–87. Springer, 1997.

[3]. Alessandri K, Sarangi BR, Gurchenkov VV, Sinha B, Kießling TR, Fetler L, Rico F, Scheuring S, Lamaze C, Simon A, et al. Cellular capsules as a tool for multicellular spheroid production and for investigating the mechanics of tumor progression in vitro. Proceedings of the National Academy of Sciences, 110(37):14843–14848, 2013.

[4]. Ambrosi D, Ateshian G, Arruda E, Cowin S, Dumais J, Goriely A, Holzapfel GA, Humphrey J, Kemkemer R, Kuhl E, Olberding J, Taberk L, and Garikipati K. Perspectives on biological growth and remodeling. Journal of the Mechanics and Physics of Solids, 59(4):863–883, 2011. [PubMed: 21532929]

[5]. Ambrosi D, Guillou A, and Di Martino E. Stress-modulated remodeling of a non-homogeneous body. Journal of Biomechanics, 39:S315, 2006.

[6]. Ambrosi D and Mollica F. On the mechanics of a growing tumor. International journal of engineering science, 40(12):1297–1316, 2002.

[7]. Ambrosi D and Mollica F. The role of stress in the growth of a multicell spheroid. Journal of mathematical biology, 48(5):477–499, 2004. [PubMed: 15133619]

[8]. Ambrosi D and Preziosi L. On the closure of mass balance models for tumor growth. Mathematical Models and Methods in Applied Sciences, 12(05):737–754, 2002.

[9]. Anderson ARA and Chaplain MAJ. Continuous and discrete mathematical models of tumor-induced angiogenesis. Bulletin of Mathematical Biology, 60(5):857–899, 1998. [PubMed: 9739618]

[10]. Araujo RP and McElwain D. A linear-elastic model of anisotropic tumour growth. European Journal of Applied Mathematics, 15(3):365–384, 2004.

[11]. Araujo RP and McElwain D. The nature of the stresses induced during tissue growth. Applied Mathematics Letters, 18(10):1081–1088, 2005.

[12]. Araujo RP and McElwain DS. A history of the study of solid tumour growth: the contribution of mathematical modelling. Bulletin of mathematical biology, 66(5):1039, 2004. [PubMed: 15294418]

[13]. Araujo RP and McElwain DS. A mixture theory for the genesis of residual stresses in growing tissues i: A general formulation. SIAM Journal on Applied Mathematics, 65(4):1261–1284, 2005.

[14]. Araujo RP and McElwain DS. A mixture theory for the genesis of residual stresses in growing tissues ii: solutions to the biphasic equations for a multicell spheroid. SIAM Journal on Applied Mathematics, 66(2):447–467, 2005.

[15]. Armstrong NJ, Painter KJ, and Sherratt JA. A continuum approach to modelling cell-cell adhesion. Journal of Theoretical Biology, 243(1):98–113, 2006. [PubMed: 16860344]

[16]. Aslan O, Cordero N, Gaubert A, and Forest S. Micromorphic approach to single crystal plasticity and damage. International Journal of Engineering Science, 49(12):1311–1325, 2011.

[17]. Astanin S and Preziosi L. Multiphase models of tumour growth In Selected topics in cancer modeling, pages 1–31. Springer, 2008.

[18]. Ateshian GA. On the theory of reactive mixtures for modeling biological growth. Biomechanics and modeling in mechanobiology, 6(6):423–445, 2007. [PubMed: 17206407]

[19]. Athale C, Mansury Y, and Deisboeck TS. Simulating the impact of a molecular 'decision-process' on cellular phenotype and multicellular patterns in brain tumors. Journal of theoretical biology, 233(4):469–481, 2005. [PubMed: 15748909]

[20]. Bedford A and Drumheller D. A variational theory of immiscible mixtures. Archive for Rational Mechanics and Analysis, 68(1):37–51, 1978.

[21]. Bilston LE, Liu Z, and Phan-Thien N. Large strain behaviour of brain tissue in shear: some experimental data and differential constitutive model. Biorheology, 38(4):335–345, 2001. [PubMed: 11673648]

[22]. Boettinger WJ, Warren JA, Beckermann C, and Karma A. Phase-field simulation of solidification. Annual review of materials research, 32(1):163–194, 2002.

[23]. Bowen RM. Theory of mixtures. Continuum physics, 3:2–129, 1976.

[24]. Bowen RM. Incompressible porous media models by use of the theory of mixtures. International Journal of Engineering Science, 18(9):1129–1148, 1980.

[25]. Breward C, Byrne H, and Lewis C. The role of cell-cell interactions in a two-phase model for avascular tumour growth. Journal of Mathematical Biology, 45(2):125–152, 2002. [PubMed: 12181602]

[26]. Butcher DT, Alliston T, and Weaver VM. A tense situation: forcing tumour progression. Nature reviews. Cancer, 9(2):108, 2009.

[27]. Buttenschoen A, Hillen T, Gerisch A, and Painter KJ. A space-jump derivation for non-local models of cell-cell adhesion and non-local chemotaxis. Journal of mathematical biology, 76(1–2):429–456, 2018. [PubMed: 28597056]

[28]. Byrne HM, King JR, McElwain DS, and Preziosi L. A two-phase model of solid tumour growth. Applied Mathematics Letters, 16(4):567–573, 2003.

[29]. Cahn JW and Hilliard JE. Free energy of a nonuniform system. i. interfacial free energy. The Journal of chemical physics, 28(2):258–267, 1958.

[30]. Cheng G, Tse J, Jain RK, and Munn LL. Micro-environmental mechanical stress controls tumor spheroid size and morphology by suppressing proliferation and inducing apoptosis in cancer cells. PLoS one, 4(2):e4632, 2009. [PubMed: 19247489]

[31]. Cheng S, Clarke EC, and Bilston LE. Rheological properties of the tissues of the central nervous system: a review. Medical Engineering and Physics, 30(10):1318–1337, 2008. [PubMed: 18614386]

[32]. Choksi R, Peletier MA, and Williams J. On the phase diagram for microphase separation of diblock copolymers: An approach via a nonlocal cahn–hilliard functional. SIAM Journal on Applied Mathematics, 69(6):1712–1738, 2009.

[33]. Cloots R, Van Dommelen J, Nyberg T, Kleiven S, and Geers M. Micromechanics of diffuse axonal injury: influence of axonal orientation and anisotropy. Biomechanics and modeling in mechanobiology, 10(3):413–422, 2011. [PubMed: 20635116]

[34]. Coleman BD and Noll W. The thermodynamics of elastic materials with heat conduction and viscosity. Archive for rational mechanics and analysis, 13(1):167–178, 1963.

[35]. Cristini V, Li X, Lowengrub JS, and Wise SM. Nonlinear simulations of solid tumor growth using a mixture model: invasion and branching. Journal of Mathematical Biology, 58(4):723, 9 2008. [PubMed: 18787827]

[36]. Dai M, Feireisl E, Rocca E, Schimperna G, and Schonbek ME. Analysis of a diffuse interface model of multispecies tumor growth. Nonlinearity, 30(4):1639, 2017.

[37]. De Boer R. Trends in continuum mechanics of porous media, volume 18 Springer Science & Business Media, 2006.

[38]. De Boer R. Theory of porous media: highlights in historical development and current state. Springer Science & Business Media, 2012.

[39]. de Rooij R and Kuhl E. Constitutive modeling of brain tissue: current perspectives. Applied Mechanics Reviews, 68(1):010801, 2016.

[40]. Demou ZN. Gene expression profiles in 3d tumor analogs indicate compressive strain differentially enhances metastatic potential. Annals of biomedical engineering, 38(11):3509–3520, 2010. [PubMed: 20559731]

[41]. Dziwnik M, Münch A, and Wagner B. An anisotropic phase-field model for solid-state dewetting and its sharp-interface limit. Nonlinearity, 30(4):1465, 2017.

[42]. Eringen AC and Ingram JD. A continuum theory of chemically reacting media-I. International Journal of Engineering Science, 3(2):197–212, 1965.

[43]. Faghihi D, Oden JT, Feng X, Lima EABF, Hormuth II DA, and Yankeelov TE. A phase-field theory for multi-constituent diffusion and deformation: Application to avascular tumor growth, 2018.

[44]. Faghihi D and Voyiadjis GZ. A thermodynamic consistent model for coupled strain-gradient plasticity with temperature. Journal of Engineering Materials and Technology, 136(1):011002, 2014.

[45]. Forest S. Micromorphic approach for gradient elasticity, viscoplasticity, and damage. Journal of Engineering Mechanics, 135(3):117–131, 2009.

[46]. Fraldi M and Carotenuto AR. Cells competition in tumor growth poroelasticity. Journal of the Mechanics and Physics of Solids, 112:345–367, 2018.

[47]. Franceschini G, Bigoni D, Regitnig P, and Holzapfel GA. Brain tissue deforms similarly to filled elastomers and follows consolidation theory. Journal of the Mechanics and Physics of Solids, 54(12):2592–2620, 2006.

[48]. Franks S and King J. Interactions between a uniformly proliferating tumour and its surroundings: uniform material properties. Mathematical medicine and biology, 20(1):47–89, 2003. [PubMed: 12974498]

[49]. Frieboes HB, Lowengrub JS, Wise S, Zheng X, Macklin P, Bearer EL, and Cristini V. Computer simulation of glioma growth and morphology. Neuroimage, 37:S59–S70, 2007. [PubMed: 17475515]

[50]. Fried E and Gurtin EM. A unified treatment of evolving interfaces accounting for small deformations and atomic transport: grain-boundaries, phase transitions, epitaxy. 2005.

[51]. Fried E and Gurtin ME. Coherent solid-state phase transitions with atomic diffusion: a thermomechanical treatment. Journal of Statistical Physics, 95(5):1361–1427, 1999.

[52]. Friedl P and Wolf K. Tumour-cell invasion and migration: diversity and escape mechanisms. Nature reviews cancer, 3(5):362, 2003. [PubMed: 12724734]

[53]. Fung Y-C. Biomechanics: mechanical properties of living tissues. Springer Science & Business Media, 2013.

[54]. Garcke H, Lam KF, Sitka E, and Styles V. A Cahn–Hilliard–Darcy model for tumour growth with chemotaxis and active transport. Mathematical Models and Methods in Applied Sciences, 26(06):1095–1148, 2016.

[55]. Garg I and Miga MI. Preliminary investigation of the inhibitory effects of mechanical stress in tumor growth. In Proc. SPIE, volume 6918, page L69182, 2008.

[56]. Garikipati K. The kinematics of biological growth. Applied Mechanics Reviews, 62(3):030801, 2009.

[57]. Garikipati K, Arruda E, Grosh K, Narayanan H, and Calve S. A continuum treatment of growth in biological tissue: the coupling of mass transport and mechanics. Journal of the Mechanics and Physics of Solids, 52(7):1595–1625, 2004.

[58]. Germain P. The method of virtual power in continuum mechanics. part 2: Microstructure. SIAM Journal on Applied Mathematics, 25(3):556–575, 1973.

[59]. Goodman M and Cowin S. A continuum theory for granular materials. Archive for Rational Mechanics and Analysis, 44(4):249–266, 1972.

[60]. Goriely A and Amar MB. On the definition and modeling of incremental, cumulative, and continuous growth laws in morphoelasticity. Biomechanics and modeling in mechanobiology, 6(5):289–296, 2007. [PubMed: 17123061]

[61]. Graziano L and Preziosi L. Mechanics in tumor growth. Modeling of biological materials, pages 263–321, 2007.

[62]. Gurtin ME. Generalized Ginzburg-Landau and Cahn-Hilliard equations based on a microforce balance. Physica D: Nonlinear Phenomena, 92(3–4):178–192, 1996.

[63]. Gurtin ME. A gradient theory of single-crystal viscoplasticity that accounts for geometrically necessary dislocations. Journal of the Mechanics and Physics of Solids, 50(1):5–32, 2002.

[64]. Gurtin ME and Anand L. A theory of strain-gradient plasticity for isotropic, plastically irrotational materials. part i: Small deformations. Journal of the Mechanics and Physics of Solids, 53(7):1624–1649, 2005.

[65]. Gurtin ME and Anand L. A theory of strain-gradient plasticity for isotropic, plastically irrotational materials. part ii: Finite deformations. International Journal of Plasticity, 21(12):2297–2318, 2005.

[66]. Gurtin ME, Fried E, and Anand L. The mechanics and thermodynamics of continua. Cambridge University Press, 2010.

[67]. Gurtin ME and Guidugli PP. The thermodynamics of constrained materials. Archive for Rational Mechanics and Analysis, 51(3):192–208, 1973.

[68]. Gurtin ME and McFadden GB. On the evolution of phase boundaries, volume 43 Springer Science & Business Media, 2012.

[69]. Gurtin ME and Williams WO. On the clausius-duhem inequality. Zeitschrift für Angewandte Mathematik und Physik (ZAMP), 17(5):626–633, 1966.

[70]. Gurtin ME and Williams WO. An axiomatic foundation for continuum thermodynamics. Archive for Rational Mechanics and Analysis, 26(2):83–117, 1967.

[71]. Hawkins-Daarud A, van der Zee KG, and Tinsley Oden J. Numerical simulation of a thermodynamically consistent four-species tumor growth model. International journal for numerical methods in biomedical engineering, 28(1):3–24, 2012. [PubMed: 25830204]

[72]. Helmlinger G, Netti PA, Lichtenbeld HC, Melder RJ, and Jain RK. Solid stress inhibits the growth of multicellular tumor spheroids. Nature biotechnology, 15(8):778–783, 1997.

[73]. Himpel G, Kuhl E, Menzel A, and Steinmann P. Computational modelling of isotropic multiplicative growth. Comp Mod Eng Sci, 8:119–134, 2005.

[74]. Hormuth DA, Weis JA, Barnes SL, Miga MI, Rericha EC, Quaranta V, and Yankeelov TE. A mechanically coupled reaction–diffusion model that incorporates intra-tumoural heterogeneity to predict in vivo glioma growth. Journal of The Royal Society Interface, 14(128), 2017.

[75]. Hrapko M, Van Dommelen J, Peters G, and Wismans J. The mechanical behaviour of brain tissue: large strain response and constitutive modelling. Biorheology, 43(5):623–636, 2006. [PubMed: 17047281]

[76]. Humphrey J and Rajagopal K. A constrained mixture model for growth and remodeling of soft tissues. Mathematical models and methods in applied sciences, 12(03):407–430, 2002.

[77]. Ingram JD and Eringen AC. A continuum theory of chemically reacting media–II constitutive equations of reacting fluid mixtures. International Journal of Engineering Science, 5(4):289–322, 1967.

[78]. Jain RK, Martin JD, and Stylianopoulos T. The role of mechanical forces in tumor growth and therapy. Annual review of biomedical engineering, 16:321–346, 2014.

[79]. Janet MT, Cheng G, Tyrrell JA, Wilcox-Adelman SA, Boucher Y, Jain RK, and Munn LL. Mechanical compression drives cancer cells toward invasive phenotype. Proceedings of the National Academy of Sciences, 109(3):911–916, 2012.

[80]. Jarrett AM, Lima EABF, Hormuth DA, McKenna MT, Feng X, Ekrut CA, Resende ACM, Brock A, and Yankeelov TE. Mathematical models of tumor cell proliferation: A review of the literature. Expert review of anticancer therapy, 18(12):1271–1286, 2018. [PubMed: 30252552]

[81]. Jenkins J. Static equilibrium of granular materials. Journal of Applied Mechanics, 42(3):603–606, 1975.

[82]. Jiang Y, Pjesivac-Grbovic J, Cantrell C, and Freyer JP. A multiscale model for avascular tumor growth. Biophysical journal, 89(6):3884–3894, 2005. [PubMed: 16199495]

[83]. Joseph D and Renardy Y. Fundamentals of two fluid mechanics, 1993.

[84]. Karagiannis GS, Poutahidis T, Erdman SE, Kirsch R, Riddell RH, and Diamandis CP. Cancer-associated fibroblasts drive the progression of metastasis through both paracrine and mechanical pressure on cancer tissue. Molecular cancer research, 10(11):1403–1418, 2012. [PubMed: 23024188]

[85]. Kaufman L, Brangwynne C, Kasza K, Filippidi E, Gordon VD, Deisboeck T, and Weitz D. Glioma expansion in collagen i matrices: analyzing collagen concentration-dependent growth and motility patterns. Biophysical journal, 89(1):635–650, 2005. [PubMed: 15849239]

[86]. Knowles J and Jakub M. Finite dynamic deformations of an incompressible elastic medium containing a spherical cavity. Archive for Rational Mechanics and Analysis, 18(5):367–378, 1965.

[87]. Koike C, McKee T, Pluen A, Ramanujan S, Burton K, Munn L, Boucher Y, and Jain R. Solid stress facilitates spheroid formation: potential involvement of hyaluronan. British journal of cancer, 86(6):947, 2002. [PubMed: 11953828]

[88]. Laird AK. Dynamics of tumour growth. British journal of cancer, 18(3):490, 1964.

[89]. Lee AA, Münch A, and Süli E. Degenerate mobilities in phase field models are insufficient to capture surface diffusion. Applied Physics Letters, 107(8):081603, 2015.

[90]. Lee AA, Munch A, and Suli E. Sharp-interface limits of the cahn–hilliard equation with degenerate mobility. SIAM Journal on Applied Mathematics, 76(2):433–456, 2016.

[91]. Levental KR, Yu H, Kass L, Lakins JN, Egeblad M, Erler JT, Fong SF, Csiszar K, Giaccia A, Weninger W, et al. Matrix crosslinking forces tumor progression by enhancing integrin signaling. Cell, 139(5):891–906, 2009. [PubMed: 19931152]

[92]. Li B, Cao Y-P, Feng X-Q, and Gao H. Surface wrinkling of mucosa induced by volumetric growth: theory, simulation and experiment. Journal of the Mechanics and Physics of Solids, 59(4):758–774, 2011.

[93]. Li B, Cao Y-P, Feng X-Q, and Gao H. Mechanics of morphological instabilities and surface wrinkling in soft materials: a review. Soft Matter, 8(21):5728–5745, 2012.

[94]. Lima EABF, Almeida RC, and Oden JT. Analysis and numerical solution of stochastic phase-field models of tumor growth. Numerical Methods for Partial Differential Equations, 31(2):552–574, 2015.

[95]. Lima EABF, Ghousifam N, Ozkan A, Oden JT, Shahmoradi A, Rylander M, Wohlmuth B, and Yankeelov T. Calibration of multi-parameter models of avascular tumor growth using time resolved microscopy data. Scientific reports, 8(1):14558, 2018. [PubMed: 30266911]

[96]. Lima EABF, Oden JT, and Almeida RC. A hybrid ten-species phase-field model of tumor growth. Mathematical Models and Methods in Applied Sciences, 24(13):2569–2599, 2014.

[97]. Lima EABF, Oden JT, Hormuth DA, Yankeelov TE, and Almeida RC. Selection, calibration, and validation of models of tumor growth. Mathematical Models and Methods in Applied Sciences, 26(12):2341–2368, 2016. [PubMed: 28827890]

[98]. Liu J. Thermodynamically consistent modeling and simulation of multiphase flows. PhD thesis, The University of Texas at Austin, 2014.

[99]. Liu J, Gomez H, Evans JA, Hughes TJ, and Landis CM. Functional entropy variables: a new methodology for deriving thermodynamically consistent algorithms for complex fluids, with

particular reference to the isothermal navier–stokes–korteweg equations. Journal of Computational Physics, 248:47–86, 2013.

[100]. Liu J, Landis CM, Gomez H, and Hughes TJ. Liquid–vapor phase transition: thermomechanical theory, entropy stable numerical formulation, and boiling simulations. Computer Methods in Applied Mechanics and Engineering, 297:476–553, 2015.

[101]. Lorenzo G, Hughes TJ, Dominguez-Frojan P, Reali A, and Gomez H. Computer simulations suggest that prostate enlargement due to benign prostatic hyperplasia mechanically impedes prostate cancer growth. Proceedings of the National Academy of Sciences, 116(4):1152–1161, 2019.

[102]. Lubarda VA and Hoger A. On the mechanics of solids with a growing mass. International journal of solids and structures, 39(18):4627–4664, 2002.

[103]. Macklin P and Edgerton ME. Agent-based cell modeling: application to breast cancer. In Multiscale Modeling of Cancer: An Integrated Experimental and Mathematical Modeling Approach, pages 206–234. Cambridge University Press, 2010.

[104]. Macklin P, Frieboes HB, Sparks JL, Ghaffarizadeh A, Friedman SH, Juarez EF, Jonckheere E, and Mumenthaler SM. Progress towards computational 3-d multicellular systems biology In Systems Biology of Tumor Microenvironment, pages 225–246. Springer, 2016.

[105]. Madireddy S, Sista B, and Vemaganti K. Bayesian calibration of hyperelastic constitutive models of soft tissue. Journal of the mechanical behavior of biomedical materials, 59:108–127, 2016. [PubMed: 26751706]

[106]. Mascheroni P, Stigliano C, Carfagna M, Boso DP, Preziosi L, Decuzzi P, and Schrefler BA. Predicting the growth of glioblastoma multiforme spheroids using a multiphase porous media model. Biomechanics and modeling in mechanobiology, 15(5):1215–1228, 2016. [PubMed: 26746883]

[107]. Mihai LA, Chin L, Janmey PA, and Goriely A. A comparison of hyperelastic constitutive models applicable to brain and fat tissues. Journal of The Royal Society Interface, 12(110), 2015.

[108]. Mills KL, Garikipati K, and Kemkemer R. Experimental characterization of tumor spheroids for studies of the energetics of tumor growth. International Journal of Materials Research, 102(7):889–895, 2011.

[109]. Mills KL, Kemkemer R, Rudraraju S, and Garikipati K. Elastic free energy drives the shape of prevascular solid tumors. PLoS One, 9(7):e103245, 2014. [PubMed: 25072702]

[110]. Mills KL, Kemkemer R, Rudraraju S, and Garikipati K. Tumor growth in agarose and collagen-agarose co-gels. Book of Abstracts-Extract, page 25, 2015.

[111]. Mills KL, Rudraraju S, Kemkemer R, and Garikipati K. Continuum physics of tumor growth. Cell and Matrix Mechanics, page 309, 2014.

[112]. Moelans N, Wendler F, and Nestler B. Comparative study of two phase-field models for grain growth. Computational Materials Science, 46(2):479–490, 2009.

[113]. Montel F, Delarue M, Elgeti J, Malaquin L, Basan M, Risler T, Cabane B, Vignjevic D, Prost J, Cappello G, et al. Stress clamp experiments on multicellular tumor spheroids. Physical review letters, 107(18):188102, 2011. [PubMed: 22107677]

[114]. Montel F, Delarue M, Elgeti J, Vignjevic D, Cappello G, and Prost J. Isotropic stress reduces cell proliferation in tumor spheroids. New Journal of Physics, 14(5):055008, 2012.

[115]. Mooney M. A theory of large elastic deformation. Journal of applied physics, 11(9):582–592, 1940.

[116]. Narayanan H, Arruda E, Grosh K, and Garikipati K. The micromechanics of fluid–solid interactions during growth in porous soft biological tissue. Biomechanics and modeling in mechanobiology, 8(3):167, 2009. [PubMed: 18470548]

[117]. Narayanan H, Verner S, Mills KL, Kemkemer R, and Garikipati K. In silico estimates of the free energy rates in growing tumor spheroids. Journal of Physics: Condensed Matter, 22(19):194122, 2010. [PubMed: 21386444]

[118]. Nunziato JW and Walsh EK. On ideal multiphase mixtures with chemical reactions and diffusion. Archive for Rational Mechanics and Analysis, 73(4):285–311, 1980.

[119]. Oden JT and Demkowicz L. Applied functional analysis. Chapman and Hall/CRC, 2010.

[120]. Oden JT, Hawkins A, and Prudhomme S. General diffuse-interface theories and an approach to predictive tumor growth modeling. Mathematical Models and Methods in Applied Sciences, 20(03):477–517, 2010.

[121]. Oden JT, Lima EABF, Almeida RC, Feng Y, Rylander MN, Fuentes D, Faghihi D, Rahman MM, DeWitt M, Gadde M, et al. Toward predictive multiscale modeling of vascular tumor growth. Archives of Computational Methods in Engineering, 23(4):735–779, 2016.

[122]. Ogden RW. Large deformation isotropic elasticity–on the correlation of theory and experiment for incompressible rubberlike solids. Proc. R. Soc. Lond. A, 326(1567):565–584, 1972.

[123]. Ogden RW. Non-linear elastic deformations. Courier Corporation, 1997.

[124]. Padera TP, Stoll BR, Tooredman JB, Capen D, di Tomaso E, and Jain RK. Pathology: cancer cells compress intratumour vessels. Nature, 427(6976):695, 2004. [PubMed: 14973470]

[125]. Papastavrou A, Steinmann P, and Kuhl E. On the mechanics of continua with boundary energies and growing surfaces. Journal of the Mechanics and Physics of Solids, 61(6):1446–1463, 2013. [PubMed: 23606760]

[126]. Passman SL, Nunziato JW, and Walsh EK. A theory of multiphase mixtures In Rational thermodynamics, pages 286–325. Springer, 1984.

[127]. Paszek MJ, Zahir N, Johnson KR, Lakins JN, Rozenberg GI, Gefen A, Reinhart-King CA, Margulies SS, Dembo M, Boettiger D, et al. Tensional homeostasis and the malignant phenotype. Cancer cell, 8(3):241–254, 2005. [PubMed: 16169468]

[128]. Paweletz N and Knierim M. Tumor-related angiogenesis. Critical reviews in oncology/hematology, 9(3):197–242, 1989. [PubMed: 2480145]

[129]. Pennacchietti S, Michieli P, Galluzzo M, Mazzone M, Giordano S, and Comoglio PM. Hypoxia promotes invasive growth by transcriptional activation of the met protooncogene. Cancer cell, 3(4):347–361, 2003. [PubMed: 12726861]

[130]. Prevost TP, Balakrishnan A, Suresh S, and Socrate S. Biomechanics of brain tissue. Acta biomaterialia, 7(1):83–95, 2011. [PubMed: 20603231]

[131]. Quaranta V, Weaver AM, Cummings PT, and Anderson AR. Mathematical modeling of cancer: the future of prognosis and treatment. Clinica Chimica Acta, 357(2):173–179, 2005.

[132]. Rajagopal KR and Tao L. Mechanics of mixtures, volume 35 World scientific, 1995.

[133]. Raman F, Scribner E, Saut O, Wenger C, Colin T, and Fathallah-Shaykh HM. Computational trials: unraveling motility phenotypes, progression patterns, and treatment options for glioblastoma multiforme. PloS one, 11(1):e0146617, 2016. [PubMed: 26756205]

[134]. Rivlin R. Large elastic deformations of isotropic materials iv. further developments of the general theory. Phil. Trans. R. Soc. Lond. A, 241(835):379–397, 1948.

[135]. Rocha HL, Almeida RC, Lima EABF, Resende ACM, Oden JT, and Yankeelov TE. A hybrid three-scale model of tumor growth. Mathematical Models and Methods in Applied Sciences, 28(01):61–93, 2018. [PubMed: 29353950]

[136]. Rodriguez EK, Hoger A, and McCulloch AD. Stress-dependent finite growth in soft elastic tissues. Journal of biomechanics, 27(4):455–467, 1994. [PubMed: 8188726]

[137]. Roose T, Chapman SJ, and Maini PK. Mathematical models of avascular tumor growth. Siam Review, 49(2):179–208, 2007.

[138]. Roose T, Netti PA, Munn LL, Boucher Y, and Jain RK. Solid stress generated by spheroid growth estimated using a linear poroelasticity model. Microvascular research, 66(3):204–212, 2003. [PubMed: 14609526]

[139]. Rudraraju S, Mills KL, Kemkemer R, and Garikipati K. Multiphysics modeling of reactions, mass transport and mechanics of tumor growth In Computer Models in Biomechanics, pages 293–303. Springer, 2013.

[140]. Sarntinoranont M, Rooney F, and Ferrari M. Interstitial stress and fluid pressure within a growing tumor. Annals of biomedical engineering, 31(3):327–335, 2003. [PubMed: 12680730]

[141]. Sherratt JA, Gourley SA, Armstrong NJ, and Painter KJ. Boundedness of solutions of a non-local reaction–diffusion model for adhesion in cell aggregation and cancer invasion. European Journal of Applied Mathematics, 20(1):123–144, 2009.

[142]. Skalak R. Growth as a finite displacement field In Proceedings of the IUTAM symposium on finite elasticity, pages 347–355. Springer, 1981.

[143]. Skalak R, Dasgupta G, Moss M, Otten E, Dullemeijer P, and Vilmann H. Analytical description of growth. Journal of Theoretical Biology, 94(3):555–577, 1982. [PubMed: 7078218]

[144]. Skalak R, Zargaryan S, Jain RK, Netti PA, and Hoger A. Compatibility and the genesis of residual stress by volumetric growth. Journal of mathematical biology, 34(8):889–914, 1996. [PubMed: 8858855]

[145]. Stefanescu DM. Thermodynamic concepts–equilibrium and nonequilibrium during solidification In Science and Engineering of Casting Solidification, pages 7–27. Springer, 2015.

[146]. Stylianopoulos T, Martin JD, Chauhan VP, Jain SR, Diop-Frimpong B, Bardeesy N, Smith BL, Ferrone CR, Hornicek FJ, Boucher Y, et al. Causes, consequences, and remedies for growth-induced solid stress in murine and human tumors. Proceedings of the National Academy of Sciences, 109(38):15101–15108, 2012.

[147]. Stylianopoulos T, Martin JD, Snuderl M, Mpekris F, Jain SR, and Jain RK. Coevolution of solid stress and interstitial fluid pressure in tumors during progression: implications for vascular collapse. Cancer research, 73(13):3833–3841, 2013. [PubMed: 23633490]

[148]. Sutherland RM. Cell and environment interactions in tumor microregions: the multicell spheroid model. Science, 240(4849):177–184, 1988. [PubMed: 2451290]

[149]. Swanson KR, Bridge C, Murray J, and Alvord EC. Virtual and real brain tumors: using mathematical modeling to quantify glioma growth and invasion. Journal of the neurological sciences, 216(1):1–10, 2003. [PubMed: 14607296]

[150]. Taber LA. Biomechanics of growth, remodeling, and morphogenesis. Evolution, 490:6, 1995.

[151]. Truesdell C. Mechanical basis of diffusion. The Journal of Chemical Physics, 37(10):2336–2344, 1962.

[152]. Truesdell C, Noll W, and Pipkin A. The non-linear field theories of mechanics. Journal of Applied Mechanics, 33:958, 1966.

[153]. Truesdell C and Toupin R. The classical field theories In Principles of Classical Mechanics and Field Theory/Prinzipien der Klassischen Mechanik und Feldtheorie, pages 226–858. Springer, 1960.

[154]. Turner S and Sherratt JA. Intercellular adhesion and cancer invasion: a discrete simulation using the extended potts model. Journal of Theoretical Biology, 216(1):85–100, 2002. [PubMed: 12076130]

[155]. Ubachs R, Schreurs P, and Geers M. A nonlocal diffuse interface model for microstructure evolution of tin–lead solder. Journal of the Mechanics and Physics of Solids, 52(8):1763–1792, 2004.

[156]. van der Gun BT, Melchers LJ, Ruiters MH, de Leij LF, McLaughlin PM, and Rots MG. Epcam in carcinogenesis: the good, the bad or the ugly. Carcinogenesis, 31(11):1913–1921, 2010. [PubMed: 20837599]

[157]. Voutouri C, Mpekris F, Papageorgis P, Odysseos AD, and Stylianopoulos T. Role of constitutive behavior and tumor-host mechanical interactions in the state of stress and growth of solid tumors. PloS one, 9(8):e104717, 2014. [PubMed: 25111061]

[158]. Voyiadjis GZ and Faghihi D. Thermo-mechanical strain gradient plasticity with energetic and dissipative length scales. International Journal of Plasticity, 30(Supplement C):218–247, 2012.

[159]. Weis JA, Miga MI, Arlinghaus LR, Li X, Abramson V, Chakravarthy AB, Pendyala P, and Yankeelov TE. Predicting the response of breast cancer to neoadjuvant therapy using a mechanically coupled reaction–diffusion model. Cancer research, 75(22):4697–4707, 2015. [PubMed: 26333809]

[160]. Weis JA, Miga MI, Arlinghaus LR, Li X, Chakravarthy AB, Abramson V, Farley J, and Yankeelov TE. A mechanically coupled reaction–diffusion model for predicting the response of breast tumors to neoadjuvant chemotherapy. Physics in medicine and biology, 58(17):5851, 2013. [PubMed: 23920113]

[161]. Weis JA, Miga MI, Arlinghaus LR, Li X, Chakravarthy AB, Abramson V, Farley J, and Yankeelov TE. A mechanically coupled reaction–diffusion model for predicting the response of

breast tumors to neoadjuvant chemotherapy. Physics in medicine and biology, 58(17):5851, 2013. [PubMed: 23920113]

[162]. Weis JA, Miga MI, and Yankeelov TE. Three-dimensional image-based mechanical modeling for predicting the response of breast cancer to neoadjuvant therapy. Computer methods in applied mechanics and engineering, 314:494–512, 2017. [PubMed: 28042181]

[163]. Weiswald L-B, Bellet D, and Dangles-Marie V. Spherical cancer models in tumor biology. Neoplasia, 17(1):1–15, 2015. [PubMed: 25622895]

[164]. Wise SM, Lowengrub JS, Frieboes HB, and Cristini V. Three-dimensional multispecies nonlinear tumor growth – I: model and numerical method. Journal of theoretical biology, 253(3):524–543, 2008. [PubMed: 18485374]

[165]. Xue S-L, Li B, Feng X-Q, and Gao H. Biochemomechanical poroelastic theory of avascular tumor growth. Journal of the Mechanics and Physics of Solids, 94:409–432, 2016.

[166]. Xue S-L, Li B, Feng X-Q, and Gao H. A non-equilibrium thermodynamic model for tumor extracellular matrix with enzymatic degradation. Journal of the Mechanics and Physics of Solids, 104:32–56, 2017.

[167]. Yankeelov TE, An G, Saut O, Luebeck EG, Popel AS, Ribba B, Vicini P, Zhou X, Weis JA, Ye K, et al. Multi-scale modeling in clinical oncology: opportunities and barriers to success. Annals of biomedical engineering, 44(9):2626–2641, 2016. [PubMed: 27384942]

[168]. Zanoni M, Piccinini F, Arienti C, Zamagni A, Santi S, Polico R, Bevilacqua A, and Tesei A. 3d tumor spheroid models for in vitro therapeutic screening: a systematic approach to enhance the biological relevance of data obtained. Scientific reports, 6:19103, 2016.

[169]. Zeng Y, Hunter A, Beyerlein I, and Koslowski M. A phase field dislocation dynamics model for a bicrystal interface system: An investigation into dislocation slip transmission across cube-on-cube interfaces. International Journal of Plasticity, 79:293–313, 2016.

[170]. Ziegler H. An attempt to generalize onsager's principle, and its significance for rheological problems. Zeitschrift für Angewandte Mathematik und Physik (ZAMP), 9(5):748–763, 1958.

[171]. Ziegler H and Hochschule ET. Some extremum principles in irreversible thermodynamics, with application to continuum mechanics. Swiss Federal Institute of Technology, 1962.

[172]. Ziegler H and Wehrli C. The derivation of constitutive relations from the free energy and the dissipation function. Advances in applied mechanics, 25:183–238, 1987.

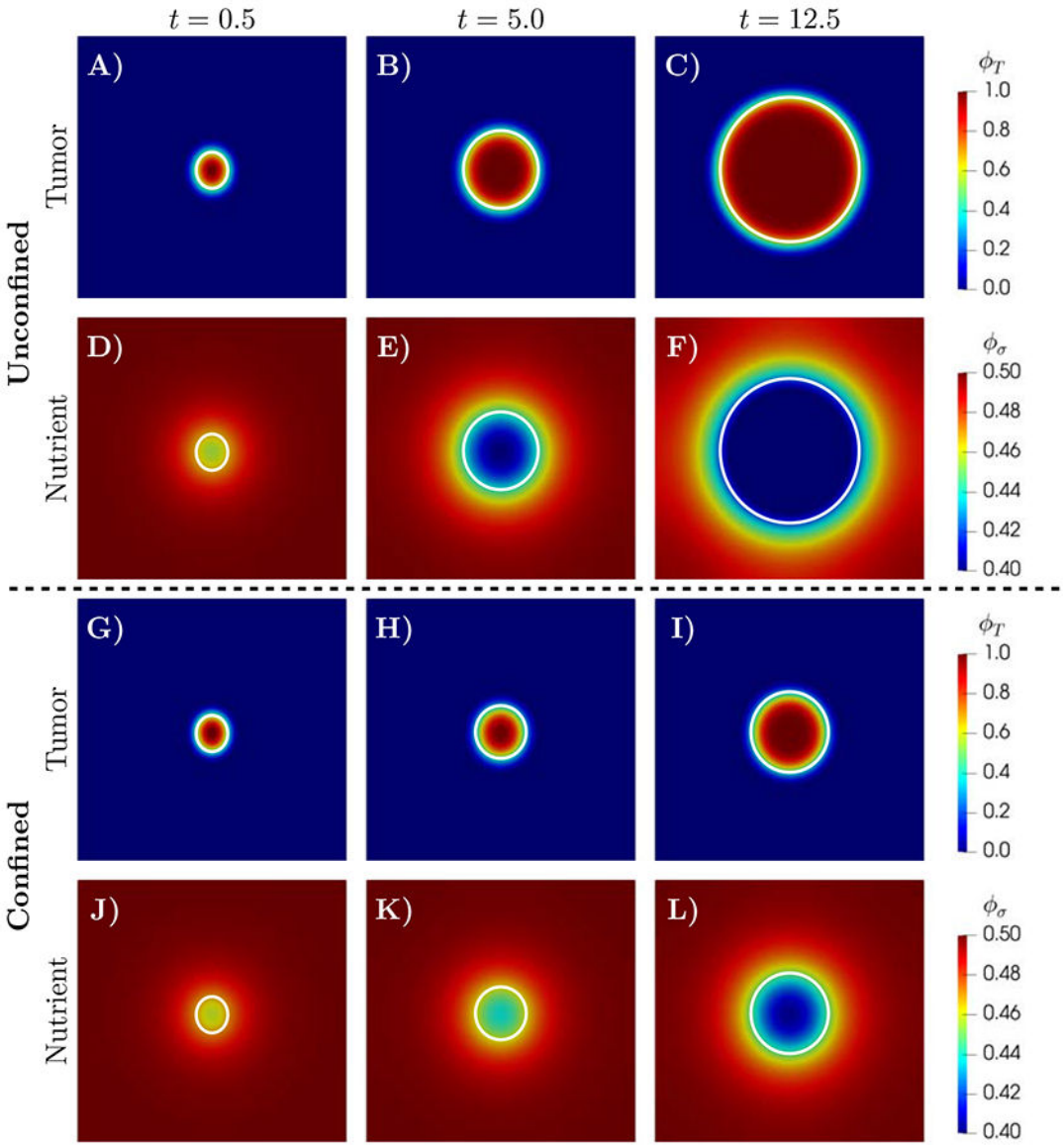

Figure 1:

Simulation results for unconfined (A-F, $\gamma_T^{pa} = \gamma_T^m = 0.0$) and confined (G-L, $\gamma_T^{pa} = \gamma_T^m = 1.0$) tumor growth with a uniform nutrient initial condition. The time evolution of tumor volume fraction, ϕ_T, and nutrient volume fraction, ϕ_σ, are shown at t=0.5, 5.0 and 12.5. In both scenarios, as the tumor grows, the nutrient is consumed. However, the mechanical feedback in the confined scenario results in a 70.82% smaller tumor size at t=12.5. The white line marks the tumor boundary.

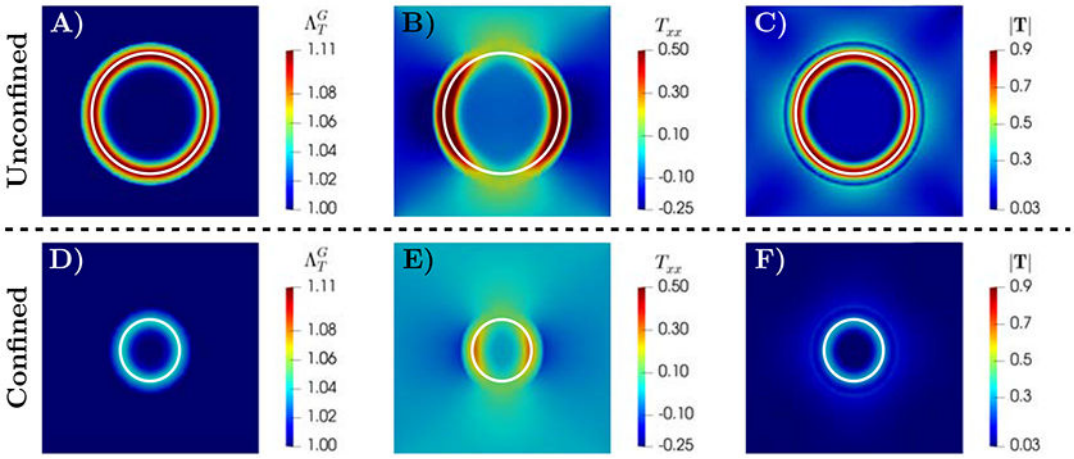

Figure 2:

Simulation results for unconfined (A-C, $\gamma_T^{pa} = \gamma_T^m = 0.0$) and confined (D-F, $\gamma_T^{pa} = \gamma_T^m = 1.0$) tumor growth with a uniform nutrient initial condition. The spatial distributions at t=12.5 are shown for: A and D) growth stretch ratio Λ_T^G, B and E) a component of Cauchy stress T_{xx}, and C and F) magnitude of Cauchy stress |**T**|. In both scenarios, the growth rate is higher at the periphery of the tumor compared to tumor interior (with the ratios of 1.12 for unconfined and 1.045 for the confined scenarios), indicating the presence of proliferative tumor cells. The white line marks the tumor boundary.

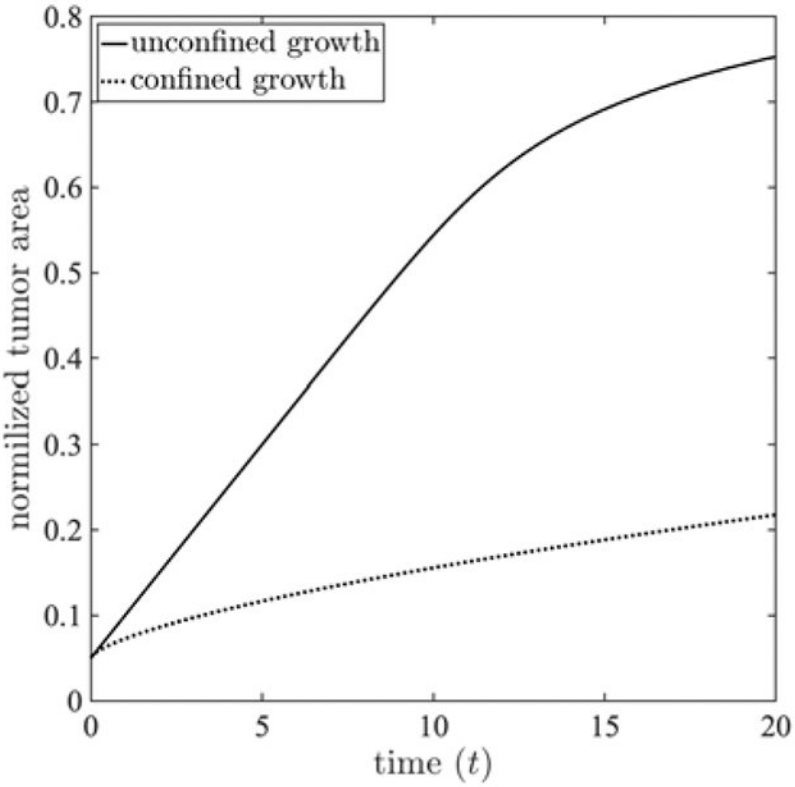

Figure 3:

The time evolution of normalized tumor area by the domain area for unconfined ($\gamma_T^{pa} = \gamma_T^m = 0.0$) and confined ($\gamma_T^{pa} = \gamma_T^m = 1.0$) tumor growth with a uniform nutrient initial condition. The mechanical feedback on cell migrations and proliferation in the confined scenario results in a lower tumor growth rate. The unconfined scenario shows an eventual reduction in tumor growth rate due to diffusion-limited supply of nutrients. For these results, a larger simulation domain $\Omega = [-2.5, 2.5]^2$ is used.

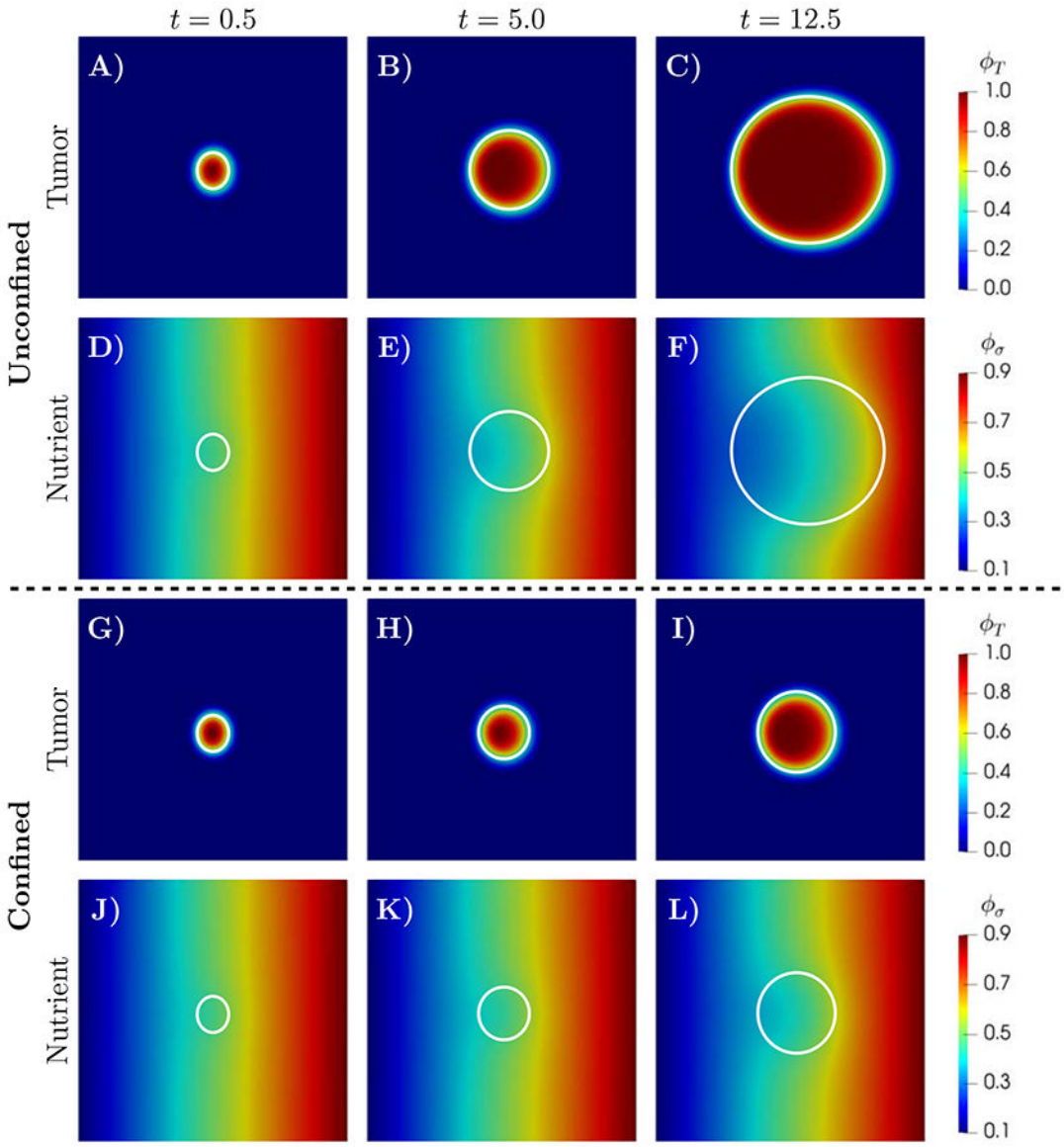

Figure 4:

Simulation results for unconfined (A-F, $\gamma_T^{pa} = \gamma_T^m = 0.0$) and confined (G-I, $\gamma_T^{pa} = \gamma_T^m = 1.0$) tumor growth with a spatially varying nutrient initial condition. The time evolution of the tumor and nutrient volume fractions, ϕ_T and ϕ_σ, respectively, are show at t=0.5, 5.0 and 12.5. In both scenarios, the tumor grows toward the higher nutrient concentration. However, the mechanical feedback in the confined scenario, results in 71.04% smaller tumor size at t=12.5. The white line marks the tumor boundary.

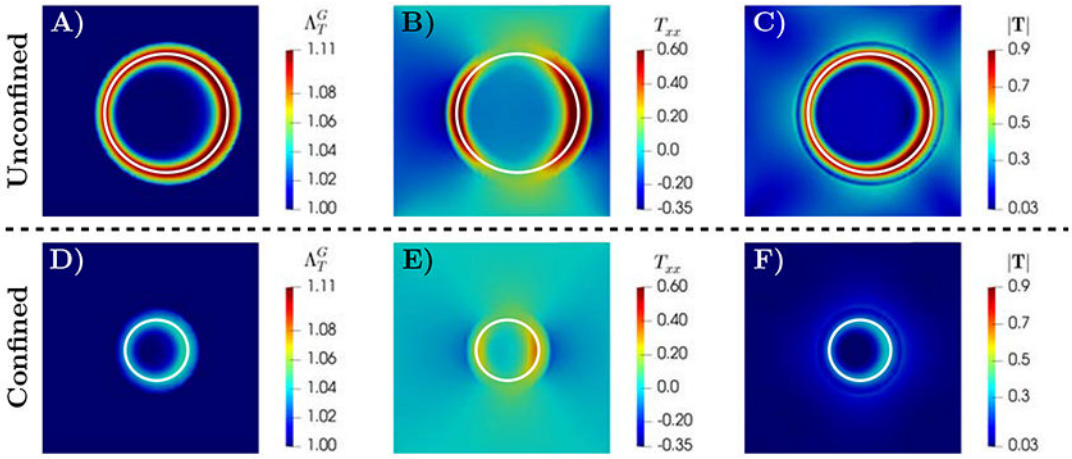

Figure 5:

Simulation results for unconfined (A-C, $\gamma_T^{pa} = \gamma_T^m = 0.0$) and confined (D-F, $\gamma_T^{pa} = \gamma_T^m = 1.0$) tumor growth with spatially varying nutrient initial condition. The spatial distributions at t = 12.5 are show for: A and D) growth stretch ratio Λ_T^G, B and E) a component of Cauchy stress T_{XX}, and C and F) magnitude of Cauchy stress |**T**|. In both scenarios, the growth rate is higher (2.75% in unconfined and 1.05% in the confined cases) on the right side of the tumor, which is closer to the higher concentration of nutrients. The white line marks the tumor boundary.

Table 1:

Set of parameters used in the numerical experiments.

Parameter	Value	Meaning
χ_0	0.15	chemotactic parameter
ϵ_T	0.01	interfacial strength among tumor cells and other species
κ	0.025	energy scale of the chemical free energy of tumor cells
δ_σ	0.01	energy scale of the chemical free energy of nutrient
λ_σ	10	coefficient of nutrient consumption by tumor cells
K_T	5.83	Bulk modulus of tumor
G_T	1.25	Shear modulus of tumor
M_σ	1	nutrient mobility
A_σ	0	viscosity coefficient of nutrient
α_T^{pa}	1.0	constant rate of the tumor cell mitosis minus the apoptosis
α_T^m	2.5	tumor cell mobility
γ_T^{pa}	0 or 1	coefficient that controls the stress feedback on tumor mass change
γ_T^m	0 or 1	coefficient that controls the stress feedback on tumor mobility